

9

**THE EFFECT OF OXYGEN PARTIAL PRESSURE ON THE EPITAXY OF
CERIUM OXIDE FILMS DEPOSITED ON NICKEL SUBSTRATES**

by

Todd S. Stefanik

B.S., Ceramic Engineering (1995)

**New York State College of Ceramics
at Alfred University**

**Submitted to the Department of Materials Science and Engineering
in Partial Fulfillment of the Requirements for the Degree of
Master of Science in Materials Science and Engineering**

at the

Massachusetts Institute of Technology

June 1998

**© 1998 Massachusetts Institute of Technology
All rights reserved**

Signature of Author.....

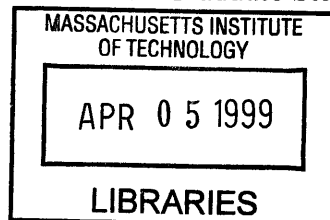
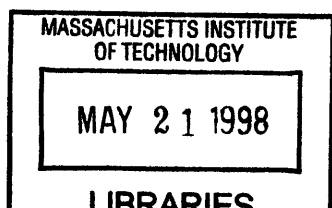
.....
**Department of Materials Science and Engineering
May 8, 1998**

Certified by.....

.....
**Michael J. Cima
Sumitomo Electric Industries Professor of Engineering
Thesis Supervisor**

Accepted by.....

.....
**Linn W. Hobbs
John F. Elliott Professor of Materials
Chairman, Departmental Committee on Graduate Students**



Science
Science

The Effect of Oxygen Partial Pressure on the Epitaxy of Cerium Oxide Films Deposited on Nickel Substrates

by

Todd S. Stefanik

Submitted to the Department of Materials Science and Engineering

on May 8th, 1998 in partial fulfillment of the requirements for the

degree of Master of Science

Abstract

Epitaxial deposition of cerium oxide thin films on nickel substrates by electron beam evaporation of cerium oxide and reactive evaporation of cerium metal was examined. Epitaxial films were produced using both techniques. The mechanisms governing each deposition technique were examined using *in-situ* electrical conductivity measurements. Electrical characterization revealed that in all cases in which epitaxial cerium oxide is deposited on nickel, the species deposited is an oxide, not a metallic phase.

The critical factor in determining the epitaxy of a cerium oxide film deposited on nickel was determined to be oxygen partial pressure. During evaporation of cerium oxide, care must be taken to ensure that the total oxygen partial pressure of the background gas does not increase enough to oxidize the substrate, thereby destroying the epitaxial surface. When determining this stability point, it is critical to account for oxygen evolved by the cerium oxide source. During reactive evaporation of cerium metal, the oxygen level must be high enough to oxidize the metallic deposition flux before it reaches the substrate or the cerium metal alloys with the nickel substrate. The oxygen level must be low enough to prevent formation of nickel oxide prior to deposition.

Reproducibility problems hinder the usefulness of reactive evaporation of cerium metal on nickel as an industrial scale production technique. Therefore, evaporation of cerium oxide for bulk production should be investigated. Although maintaining a sufficiently low oxygen partial pressure during evaporation of cerium oxide is not trivial, maintaining the oxygen partial pressure both high enough to oxidize cerium and low enough to prevent nickel oxide formation during reactive evaporation requires more stringent control than that necessary for oxide evaporation.

Thesis Supervisor: Michael J. Cima

Title: Sumitomo Electric Industries Professor of Engineering

TABLE OF CONTENTS

	<u>Page</u>
TITLE PAGE	1
ABSTRACT	2
TABLE OF CONTENTS	3
LIST OF FIGURES	5
ACKNOWLEDGMENTS	9
CHAPTER 1: INTRODUCTION	10
Superconductor material systems	10
Long length conductors	11
<i>Epitaxial films</i>	11
<i>Ion beam assisted deposition</i>	11
<i>Deformation texturing</i>	12
Buffer layer architectures	13
<i>Purpose of the buffer</i>	13
<i>Noble metals</i>	14
<i>Direct oxide deposition</i>	14
Thesis motivation	15
CHAPTER 2: EXPERIMENTS	16
Processing	16
<i>Substrates</i>	16
<i>Deposition chamber</i>	17
<i>Electron beam evaporator</i>	20
<i>Deposition conditions</i>	23
Characterization	23
<i>Deposition rate and film thickness</i>	23
<i>Crystallographic orientation</i>	25
CHAPTER 3: RESULTS	27
Crystallographic orientation	27
<i>Deposition from cerium on nickel</i>	27
<i>Deposition from oxide on nickel</i>	27
<i>Deposition on oxides</i>	30

Reproducibility issues	30
<i>Epitaxial Reproducibility</i>	30
<i>Sources of variation</i>	34
<i>Experimental evidence for the variation of background gas composition</i>	36
Film thickness calculations	39
 CHAPTER 4: DISCUSSION AND TESTING OF MECHANISMS	 43
Wetting angle mechanism	43
<i>Reduced CeO₂ deposition</i>	46
<i>Thermodynamics of reduced CeO₂ deposition</i>	48
Electrical characterization	48
<i>Experimental setup</i>	50
<i>Control depositions</i>	52
<i>Electrical response during epitaxial depositions from cerium</i>	56
<i>Electrical response during deposition from reduced CeO₂</i>	58
Substrate contamination mechanism	60
<i>Thermodynamics of nickel oxide formation/reduction</i>	60
<i>Depositions from CeO₂ after purging with forming gas</i>	61
<i>Oxygen evolution from the source</i>	61
Description of active mechanisms	65
 CHAPTER 5: CONCLUSIONS	 68
 APPENDIX A: UV/VIS THICKNESS MACRO	 70
 APPENDIX B: OXYGEN EVOLUTION FROM A CeO ₂ SOURCE	 101
 APPENDIX C: NICKEL OXIDE STABILITY DURING CeO ₂ DEPOSITION	 104
 APPENDIX D: OXYGEN FLOW NECESSARY TO OXIDIZE CERIUM DURING METALLIC DEPOSITION	 106
 BIBLIOGRAPHY	 108

LIST OF FIGURES

Figure #		Page #
<u>Chapter 2</u>		
2.1	Diagram of the clamping system used to mechanically mount nickel substrates for deposition.	18
2.2	Two shutter configurations possible when performing depositions. The open/closed configuration (a) was used to deposit several films of different thickness during the same deposition. The slot configuration (b) was used to deposit multiple films at different times during a deposition.	19
2.3	Chamber pressure as a function of gas flow at the control ion gauge (located beneath the high vacuum valve) and at the top of the chamber.	21
2.4	A schematic of the deposition chamber used during this study.	22
2.5	A typical UV/Vis transmission spectrum from a CeO ₂ film on silica glass showing curve fits generated during calculation of film thickness.	24
2.6	The arrangement of (200) and (111) poles in a cubic material such as CeO ₂ or nickel is shown in (a). Shown in (b) and (c) are the experimental setups for $\theta/2\theta$ scans and β scans, respectively. The angles θ , 2θ , β , and χ are identified.	26
<u>Chapter 3</u>		
3.1	Diffraction patterns of a CeO ₂ film deposited on nickel from a cerium metal source. A $\theta/2\theta$ pattern is shown in (a). The (111) β scans of the nickel substrate and epitaxial CeO ₂ film are shown in (b).	28

3.2	<p>$\theta/2\theta$ diffraction pattern for a CeO_2 film deposited on a nickel substrate from a CeO_2 source (a). Shown in (b) is the (200) β scan of the CeO_2 film.</p>	29
3.3	<p>Diffraction patterns of a CeO_2 film deposited on LaAlO_3 from a cerium metal source. Depicted in (a) is a $\theta/2\theta$ scan, while (b) shows the (111) CeO_2 β scan.</p>	31
3.4	<p>Diffraction patterns of a CeO_2 film deposited on LaAlO_3 from a CeO_2 source. The $\theta/2\theta$ scan is shown in (a). The (111) CeO_2 β scan is shown in (b).</p>	32
3.5	<p>The $\theta/2\theta$ scans shown demonstrate the lack of reproducibility in CeO_2 films deposited by reactive evaporation of cerium metal on single crystal nickel substrates. All three films were processed under the same conditions (1 $\text{\AA}/\text{s}$, 650°C, 1-2 sccm $\text{Ar}/5\%\text{H}_2$). The resulting films demonstrated (200) epitaxial alignment, (111) wire texture, and alloying of the cerium metal with the nickel substrate, respectively.</p>	33
3.6	<p>The $\theta/2\theta$ scans of CeO_2 films on LaAlO_3 substrates demonstrate a lack of reproducibility of epitaxy when depositing from a cerium metal source. Oxygen content of the background gas increases from the top scan to the bottom scan, yet only the film processed in a gas composition of intermediate oxygen partial pressure exhibits a polycrystalline component.</p>	35
3.7	<p>CeO_2 films deposited on nickel substrates from a cerium metal source undergo epitaxial growth at low film thickness, but lose this epitaxial relationship as film thickness increases, as indicated by X-ray $\theta/2\theta$ diffraction patterns.</p>	37
3.8	<p>CeO_2 films deposited from a CeO_2 source maintain an epitaxial relationship to the substrate, independent of film thickness, as indicated by X-ray $\theta/2\theta$ patterns. The films were deposited on nickel substrates capped with a thin epitaxial layer of CeO_2 deposited from cerium metal.</p>	38

3.9 X-ray $\theta/2\theta$ patterns for two films deposited on nickel from a cerium metal source. The first film was deposited immediately after the cerium source was conditioned, while the second film was deposited after three hours of evaporation. The first film exhibits (200) epitaxial CeO_2 , while the second shows evidence of alloying between the cerium metal and nickel substrate. 40

3.10 The figure shows average deposition rates for CeO_2 films deposited on silica glass substrates as calculated from optical thickness measurements as a function of total film thickness. The deposition rate programmed into the thickness monitor was 1.0 \AA/s , while the actual deposition rate achieved was 0.91 \AA/s . 42

Chapter 4

4.1 Surface contact area of a film deposited on a flat substrate varies as a function of the wetting angle (ϕ) of the deposited species on the substrate material. For high wetting angles, as depicted in (a), there is very little substrate contact, hindering epitaxial growth. For low wetting angles (b), substrate contact area is much higher, making epitaxial growth more probable. 44

4.2 CeO_2 film deposited on a glass substrate by reactive evaporation of cerium metal. The favored alignment when no epitaxial relationship with the substrate exists is (111) wire texture, as indicated by the $\theta/2\theta$ scan (a) and (200) β scan (b) shown. 45

4.3 X-ray $\theta/2\theta$ and (111) β scans of a CeO_2 film deposited from a CeO_2 source on a nickel substrate ((a) and (b), respectively). The CeO_2 source was conditioned in forming gas, then excess oxygen in the chamber was removed using cerium metal as a getter prior to deposition from the pre-conditioned CeO_2 source. The diffraction data indicate that the film grew epitaxially on the nickel substrate. 47

4.4	Ellingham diagram for NiO and CeO ₂ . The stability of these oxides as a function of temperature and gas composition may be read from the diagram.	49
4.5	A schematic of the substrate geometry (a) and electrical circuit (b) used to perform <i>in-situ</i> conductivity measurements of films during deposition.	51
4.6	Voltage response of films deposited from cerium metal after a long cerium metal purge of the chamber. 1000Å of material was deposited in 5 sccm forming gas.	53
4.7	Voltage response of films deposited from CeO ₂ in ambient atmosphere (no gas flowing).	55
4.8	Voltage response of films deposited from cerium metal in a background gas composition consisting of 0.7 sccm Ar/5%H ₂ + 0.3 sccm Ar/8%O ₂ .	57
4.9	Voltage response of films deposited from CeO ₂ after conditioning the CeO ₂ source in forming gas and removing residual oxygen from the chamber using cerium metal as a getter.	59
4.10	X-ray $\theta/2\theta$ scans of films deposited on nickel from CeO ₂ before and after purging the chamber with 12 sccm forming gas for 6 hours (pressure during purge $\sim 3 \times 10^{-4}$ mm Hg). Films were deposited in a background of 1 sccm forming gas.	62
4.11	X-ray $\theta/2\theta$ scans of films deposited from CeO ₂ before and after purging the chamber with 12 sccm forming gas for 12 hours. The chamber was not pumped during this purge, resulting in a rise of background pressure to approximately 160 mm Hg. Films were deposited in a background of 5 sccm forming gas.	63

ACKNOWLEDGEMENTS

The last three years working toward this degree have been quite an adventure. There are several people who have been instrumental in shaping my graduate experience, and I'd like to take this opportunity to recognize their contributions.

Thank you to Michael Cima for the opportunity to work on an interesting, challenging, technically relevant engineering problem. The time I've spent in the CPRL has been a stimulating learning experience. Working under Michael's supervision I have both gained a tremendous amount of technical knowledge and furthered my development as a research scientist.

I am indebted to Jack Smith for his insight and assistance during the last two years. The unique perspectives and ways of thinking about problems he has shared have not only led to many of the experimental results in this thesis, they have provided an example which strengthened my own problem solving skills as well. In addition, he's played a pivotal role in such key activities as camera discussions, ski trips, and lunch. I consider myself fortunate to have known Jack both as a colleague and as a good friend.

Thank you to Neville Sonnenberg and Kevin Ressler for "showing me the ropes." I knew absolutely nothing about vacuum processing when I started this project, and you managed to give me enough training and experience so that I was able "fly solo" for the last year and a half. I have no doubt that without your help my experience would have been far less productive.

Thank you to Barbara Layne, Lenny Rigione and John Centorino for keeping the CPRL running as smoothly as it does. All your efforts ranging from juggling schedules to evicting equipment gremlins to keeping the LN₂ flowing are appreciated.

Surviving grad school is a group effort; having friends to lean on is critical. Thank you to all the CPRL'ers for your thoughtfulness, support, and friendship. I couldn't have asked for a better bunch of people to work with.

Outside lab, Lutheran/Episcopal Ministries and intramural sports have been a significant part of my life. Thanks to everyone involved for making those activities the wonderful stress relievers that they were to me. Also deserving mention are my roommates, Anil and Dave, for your support and tolerance of all my idiosyncrasies and odd hours. I've valued your company and your friendship throughout the past several years.

Thank you to Kathye, Jack, Betty, and Ron for providing a "home away from home" for me to go to when I've managed to weasel in a little bit of free time. It's been reassuring to know that you're there when I need ya'.

Finally, thank you to my brothers and to my parents. Amidst the turmoil of everyday life, you've been the rock that I know will always be there to fall back on. You've provided both inspiration and a wonderful example to follow. I know I wouldn't be where I am today without your love, strength and support.

Thanks be to God!!!

CHAPTER 1: INTRODUCTION

Superconductor material systems

Superconductivity is a material property which has been known for many years. The conduction of electricity with zero resistance was first observed in metallic mercury by Onnes in 1911. Liquid helium refrigeration is necessary to observe superconductivity in metallic systems, however. Metallic superconductors have been exploited for some applications such as MRI magnets coils, but widespread use has been limited by the extremely low temperatures required to make these systems superconductive.¹

Bednorz and Muller first observed “high temperature” superconductivity in barium lanthanum cuprate at temperatures exceeding 30K in 1986.² The real breakthrough came in 1987 when Wu et al. observed superconductivity in yttrium barium cuprate (YBCO) at temperatures greater than 90K. This discovery allowed the use of liquid nitrogen cooling rather than liquid helium refrigeration, an important step toward the wide-spread use of superconductive materials.³ A great deal of research since 1987 has focused on processing YBCO for use in high temperature superconducting applications including superconductive leads for use in electronic packaging, power transfer applications, transformer windings, magnet windings, etc.^{1,4,5}

One of the primary obstacles hindering the widespread use of YBCO is the weak-link behavior between grains in a polycrystalline oxide sample. High angle grain boundaries significantly degrade the critical current density of a superconductor, that is, the amount of current which can be carried per unit area prior to a reversion to normal

conduction.⁶ It is necessary to eliminate such high angle grain boundaries and produce a microstructure which exhibits a high degree of crystallographic orientation in order to achieve the high critical current densities possible in the YBCO system (several MA/cm²).⁷

Long length conductors

Epitaxial films

One promising route for production of long lengths of biaxially oriented, high critical current density YBCO entails epitaxial thin film deposition. The grains of such a film are crystallographically oriented both with respect to the substrate normal and in the plane of the film, yielding a system with few very few high angle grain boundaries. Critical current densities of several MA/cm² have been reported in very thin (<0.1μm) films, and 1MA/cm² is typical for thicker films (0.5-1.0μm).⁷⁻⁹ Such a production technique requires long lengths of crystallographically oriented substrate material. Production of single crystal substrates in long lengths, like direct growth of single crystal YBCO, is not feasible on an industrial scale. The technological difficulties and resulting expense associated with current single crystal growth techniques prohibit their use for HTSC applications.

Ion beam assisted deposition

Yu *et al.* found that when niobium films were deposited on amorphous silica glass substrates with an assisting ion beam impinging on the substrate at an oblique angle, the resulting film demonstrated biaxial alignment in which specific crystallographic planes preferentially oriented themselves with respect to the assisting ion beam.¹⁰ This ion beam

assisted deposition (IBAD) technique received much attention as a method of producing long lengths of oriented buffer layers for use as epitaxial superconductor substrates.¹¹⁻¹⁴ The oriented buffer layers (most often yttria stabilized zirconia) could be deposited on readily available polycrystalline metal substrates, then superconductor could be grown on these buffers. Critical current densities on the order of 10^6 A/cm² were achieved using such a deposition architecture.¹² Unfortunately, deposition of the buffer layer material via IBAD is a relatively slow process since much of the deposited material is etched away by the assisting ion beam, and film thickness must typically be quite thick in order to achieve a well defined biaxially oriented structure.¹⁵ IBAD has fallen out of favor for production of superconducting ribbon substrates as a result. Wang et al. recently found that ion beam assisted deposition of MgO requires only a few hundred angstroms of material to achieve very good biaxial orientation. This discovery has renewed interest in IBAD for superconductor buffer layer production.¹⁶

Deformation texturing

Researchers at Oak Ridge National Laboratories (ORNL) recently discovered that the texture induced in an FCC metal during a rolling operation could be optimized by thermal processing to produce a biaxially aligned polycrystalline metal tape, suitable for successive epitaxial deposition. This process, known as deformation texturing or rolling assisted biaxially aligned substrate (RABiTS) processing is capable of producing long lengths of material very quickly relative to vacuum deposition techniques. It is an appealing process for industrial scale production of substrates for superconducting ribbon as a result.¹⁷

Buffer layer architectures

Purpose of the buffer

Unfortunately, deposition of YBCO directly on a deformation textured substrate is not possible. YBCO reacts with the substrate material during high temperature superconductor processing. The resulting contamination significantly degrades the electrical performance of the oxide superconductor.¹⁸ An epitaxial buffer layer must be deposited between the substrate and the superconductor in order to prevent such contamination. This layer must not only prevent with reaction and/or contamination of both the substrate and superconductor during high temperature processing, it must also demonstrate a lattice match to both the substrate and superconductor so that epitaxy may be maintained.

Creating a buffer layer capable of both preventing reaction and maintaining epitaxy has proven to be a rather difficult task. Several architectures have been attempted, but few have proved functional.^{18,19} One difficulty has been that the metal substrate to be coated (to date, pure nickel) readily oxidizes. An oxide must be deposited on the nickel without oxidizing the substrate prior to deposition. The buffer will not maintain an epitaxial relationship to the deformation textured substrate if oxide is present on the surface of the metal prior to buffer layer deposition. Controlling oxygen level in the chamber during deposition such that the substrate does not oxidize but stoichiometric buffer material is deposited becomes a difficult task.

Noble metals

One approach attempted by researchers at ORNL has been to coat the reactive metal substrate first with a noble metal, such as palladium or platinum, then deposit buffer layer oxides on these stable metals. Oxide may be deposited without the concern that the substrate will oxidize, since the surface of the substrate has been coated with a non reactive material. A significant problem arises with this method, however, in that the noble metal diffuses into the nickel substrate at high temperatures. As the noble metal diffuses into the metal substrate, it is no longer capable of preventing oxidation of the nickel which diffuses through from the underlying substrate. This makes deposition of oxide on top of the noble metal difficult, since oxide deposition is generally optimized via high substrate temperatures. Interdiffusion of the metals is inevitable, although such depositions are possible. An oxide layer must be deposited soon after heating the substrates so that oxidation of the substrate prior to deposition does not destroy the epitaxial metal surface. ORNL has demonstrated an epitaxial Ni/Pd/CeO₂ architecture, but did not report a critical current density for a YBCO superconductor layer deposited on such a buffer.¹⁸ Our efforts to reproduce the epitaxial architecture by evaporation have not been successful.

Direct oxide deposition

ORNL has also experimented with buffer layers of CeO₂ deposited directly on nickel via RF sputtering. CeO₂ is stable when such deposition is carried out in an ambient atmosphere of forming gas (Ar/4%H₂), but NiO is not. An initial layer of CeO₂ was grown in this forming gas atmosphere, then, once the nickel surface was coated, the atmosphere was changed to Ar/10%O₂ to ensure that stoichiometric CeO₂ was deposited for the bulk of

the film thickness. A layer of yttria stabilized zirconia (YSZ) was then deposited on this epitaxial CeO₂ layer, and YBCO was deposited via pulsed laser deposition on the buffer layer architecture. A critical current density of 7×10^5 A/cm² was achieved on this architecture.¹⁹

Similar architectures have also been deposited via electron beam evaporation. It was necessary to use a cerium metal source for the deposition in order to obtain an epitaxial film, rather than a CeO₂ source. Deposition is carried out in an atmosphere of forming gas. This leaves no source of oxygen to oxidize the cerium metal other than degassing from the chamber walls (most likely from water) or system leaks. Nonetheless, this background oxygen was apparently enough to oxidize the cerium metal to CeO₂.¹⁸

Thesis motivation

Epitaxial buffer layer deposition on nickel by electron beam evaporation has been repeated. The deposition of the CeO₂ layer from the cerium metal source is not well understood, however. Not only is it a process understood only on an empirical basis, it does not consistently produce an epitaxial CeO₂ film. Results ranging from biaxially aligned epitaxial film to randomly oriented film to nickel/cerium alloys have been obtained through relatively small changes in deposition conditions. A better understanding of this reactive evaporation process should allow more effective control over the deposition, a step which will be critical if the process is to be employed for the industrial scale production of oriented substrates for HTSC applications.

CHAPTER 2: EXPERIMENTS

Processing

Substrates

Cerium oxide films were deposited on several types of substrates during this study. Deformation textured nickel and single crystal nickel substrates were provided by American Superconductor Corporation.²⁰ Single crystal lanthanum aluminate (LaAlO_3) was purchased from Applied Technologies in the form of 2" diameter, 0.020" thick wafers.²¹ Silica glass substrates were purchased in the form of 1" by 3" by 1mm microscope slides.²² The deformation textured nickel substrates were approximately 0.25" wide as received, and were cut to length with a pair of hand shears. Lanthanum aluminate and silica substrates were mounted to a graphite block using Crystalbond²³ then cut to size using a Bronwill high speed saw²⁴ and a Beuhler diamond blade with a 0.012" kerf.²⁵ Most substrates used were approximately 0.25" by 0.25".

Oxide substrates were ultrasonically cleaned for approximately five minutes each in chloroform, then acetone, then methanol. Deformation textured nickel substrates were wiped with acetone and methanol. All substrates were visually inspected under an Olympus BH-2 microscope at 37.5X.²⁶ The substrate was wiped again with methanol if the surface was contaminated with dust.

Oxide substrates were pasted to a 2" by 2" by 0.25" stainless steel block using high purity silver paste.²⁷ The block was then placed in a Neytech oven²⁸ and slowly heated in air to burn off any organics in the paste. The heating schedule for such a burnout was

1°C/min to 220°C for 2 hours, then 2°C/min to 400°C for 2 hours. Nickel substrates could not be pasted to the block in this fashion, since the burnout step would have oxidized the surface of the substrate. Instead, clamps were fashioned and holes drilled and tapped into the mounting block such that the nickel substrates could be mechanically attached to the stainless steel block. Stainless steel shim stock was used to hold the substrate flat against the substrate block in an effort to ensure good thermal contact. See figure 2.1.

Occasionally, an oxide substrate was clamped in the manner described above. If this mounting method was employed, a layer of silver paint²⁹ was used between the substrate and block to ensure good thermal contact.

Deposition chamber

The stainless steel substrate block was bolted into the deposition chamber. A 1.75” circular Boralectric heater³⁰ was in direct contact with the back of the sample block. Two inconel sheathed thermocouples³¹ were embedded in the mounting block. One thermocouple was attached to an Omega CN-2010 PID temperature controller, the other to a digital thermometer as a redundant monitor.³¹ A shutter was constructed such that portions of the substrate block could be exposed to deposition while other portions remained covered. Two configurations were available for shuttering samples including a slot shutter and an open/closed shutter. See figure 2.2 for a diagrams of the shutter setup. This shutter was useful both during initial conditioning of the electron gun source material and when several depositions were to be performed over extended periods of time. Using the slot shutter, several films could be deposited during a long electron gun run to test the effect of conditioning time on the resulting film. Using the open/closed shutter

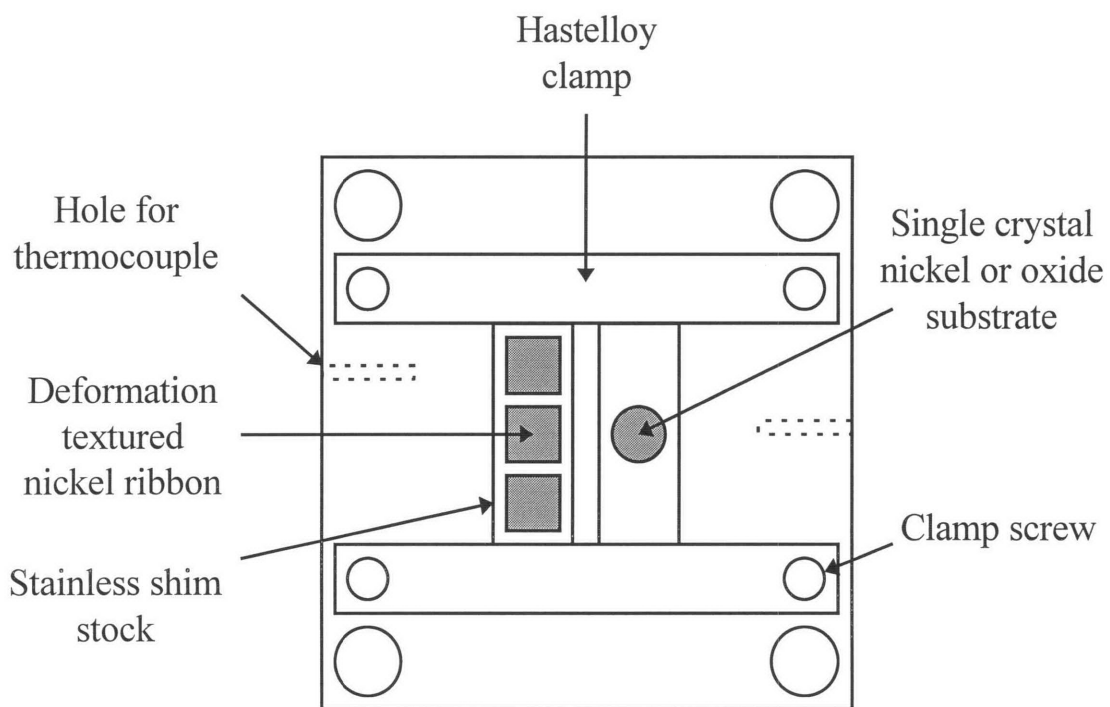
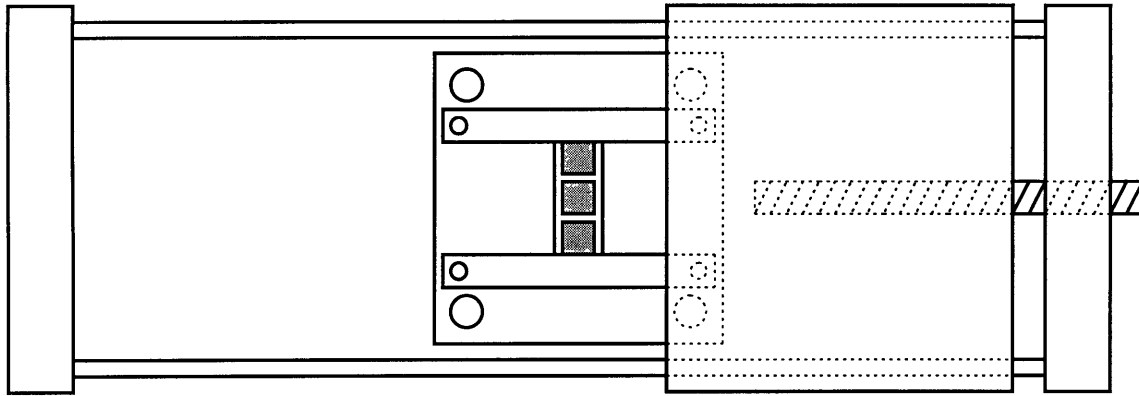
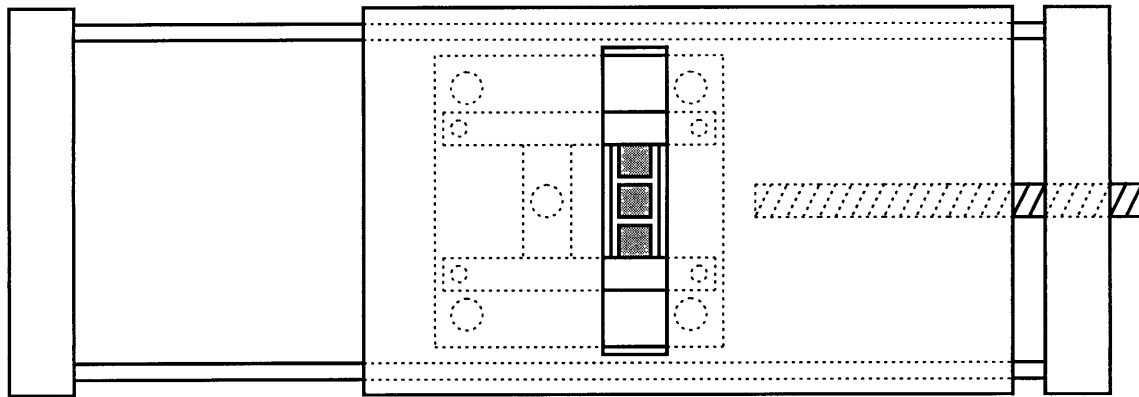


Figure 2.1. Diagram of the clamping system used to mechanically mount nickel substrates for deposition.



(a)



(b)

Figure 2.2. Two shutter configurations possible when performing depositions. The open/closed configuration (a) was used to deposit several films of different thickness during the same deposition. The slot configuration (b) was used to deposit multiple films at different times during a deposition.

configuration, films of several different thicknesses could be deposited in the same run, ensuring that deposition conditions were the same for all films in the thickness series.

The vacuum chamber was diffusion pumped by a Varian VHS-250 pump with a liquid nitrogen cold trap.³² Base pressure for the chamber was approximately 2×10^{-7} mm Hg, as read by a Varian Sen-Torr gauge controller³² and a broad range ionization tube³³ located under the gate valve of the chamber. The actual pressure in the chamber is known to be significantly higher than that read under the gate valve. Figure 2.3 shows a plot depicting the difference between the pressure read by the ion gauge and the pressure at the top of the deposition chamber as a function of gas total gas flow. All pressures reported are pressures as read from the ion gauge located beneath the high vacuum valve in the chamber. There was no load lock on the chamber; it was vented to atmosphere between samples. Gasses could be introduced into the chamber through gas leads installed to an ion source and plasma bridge neutralizer near the base of the chamber. Note that the ion source was not powered during any of the depositions presented in this work. Flow rates were controlled by an Edwards mass flow controller and valves.³⁴ See figure 2.4 for a chamber schematic.

Electron beam evaporator

Depositions were performed using a STIH-270-M electron gun with a four pocket rotating water cooled copper crucible.³⁵ The gun was powered by an Airco-Temesal CV-14 power supply.³⁵ Deposition was monitored and controlled by a quartz crystal monitor and a Sycon STC-200 rate controller.³⁶ Both cerium metal³⁷ and CeO_2 grog³⁸ sources were placed directly in the copper crucible of the electron gun (no crucible liner was used).

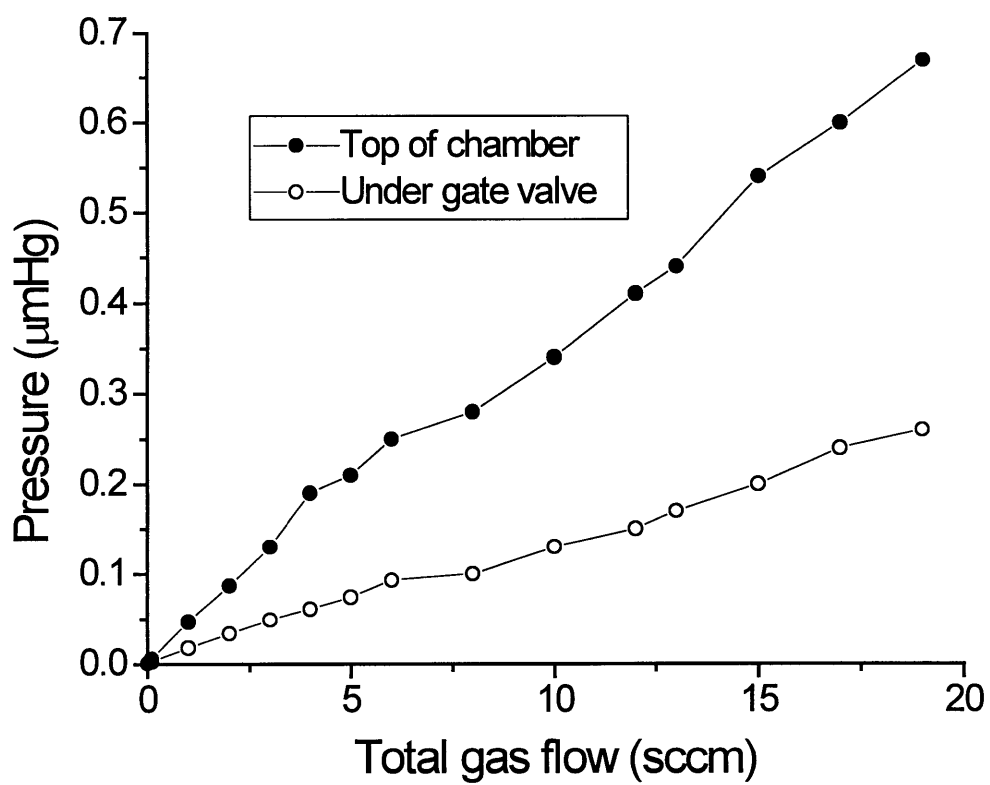


Figure 2.3. Chamber pressure as a function of gas flow at the control ion gauge (located beneath the high vacuum valve) and at the top of the chamber.

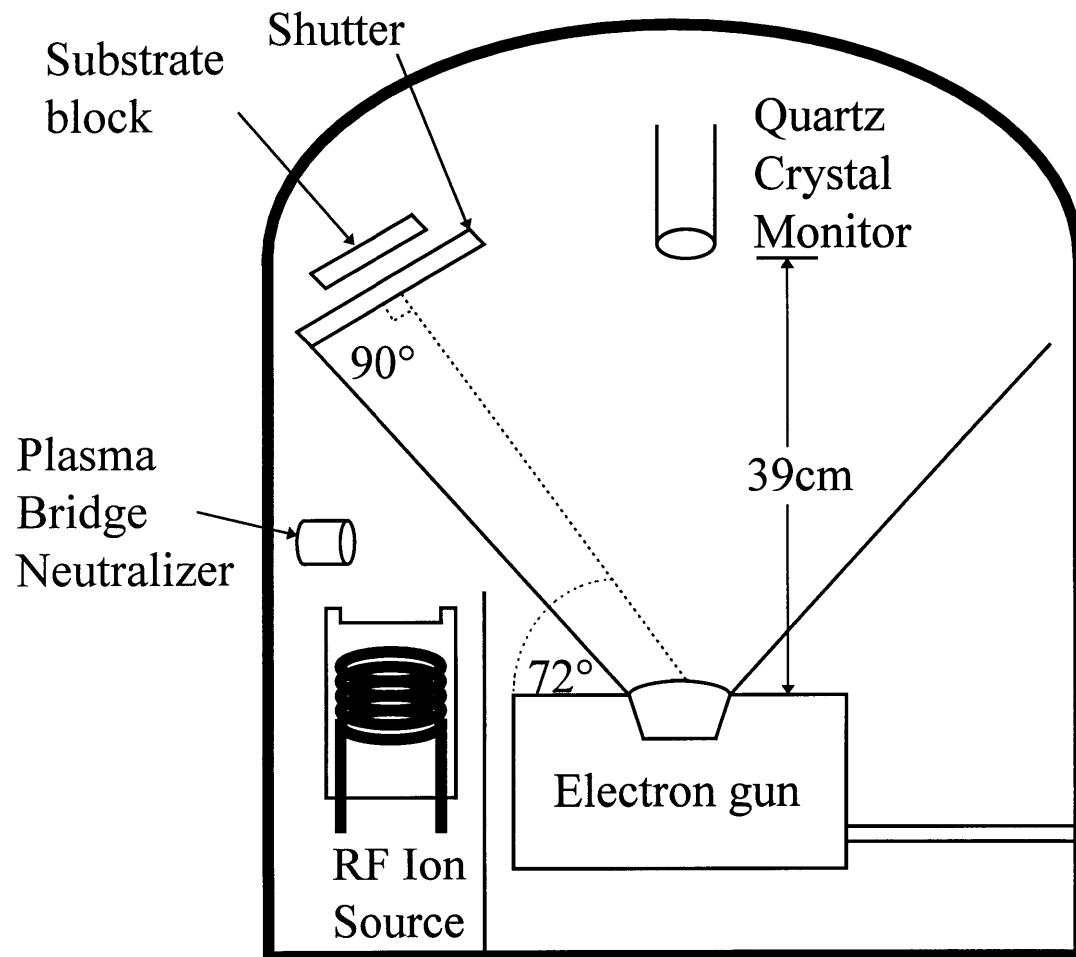


Figure 2.4. A schematic of the deposition chamber used during this study.

Deposition conditions

All depositions were performed at 650°C. Deposition rates were set to 0.5 or 1.0 Å/s as read by the quartz crystal monitor. Average deposition rates were calculated from optical thickness measurements performed after deposition. Gas compositions were varied by mixing separate flows of forming gas (Ar/5%H₂) and Ar/O₂ (typically Ar/8%O₂) into the chamber concurrently. Total gas flow varied from 0 to 5 sccm, depending on the desired deposition conditions. Pressure during deposition was typically between 10⁻⁶ to 10⁻⁴ mm Hg depending on the total gas flow to the chamber.

Characterization

Deposition rate and film thickness

Film thicknesses were calculated from interference spectra collected using a Beckman DU-640 UV/Vis spectrophotometer.³⁹ A typical transmission spectrum is shown in figure 2.5. The thickness of the film may be calculated using the spacing of the transmission minima and maxima, the transmission values at those extremes, and the index of refraction of the substrate material, as described by Swanepoel.⁴⁰ A macro was written to process such spectra in Microsoft Excel version 7.0 using Visual Basic for Applications.⁴¹ The macro identifies the extrema in the spectrum, ports the data to an external curve fitting program (Curve Expert⁴²), then uses the curve fits of the envelopes of the spectrum to calculate a film thickness. See Appendix A for the actual macro code used. The method can be accurate to less than 1% of the total film thickness, as described by Swanepoel. Mounting of the sample in the UV/Vis spectrophotometer and

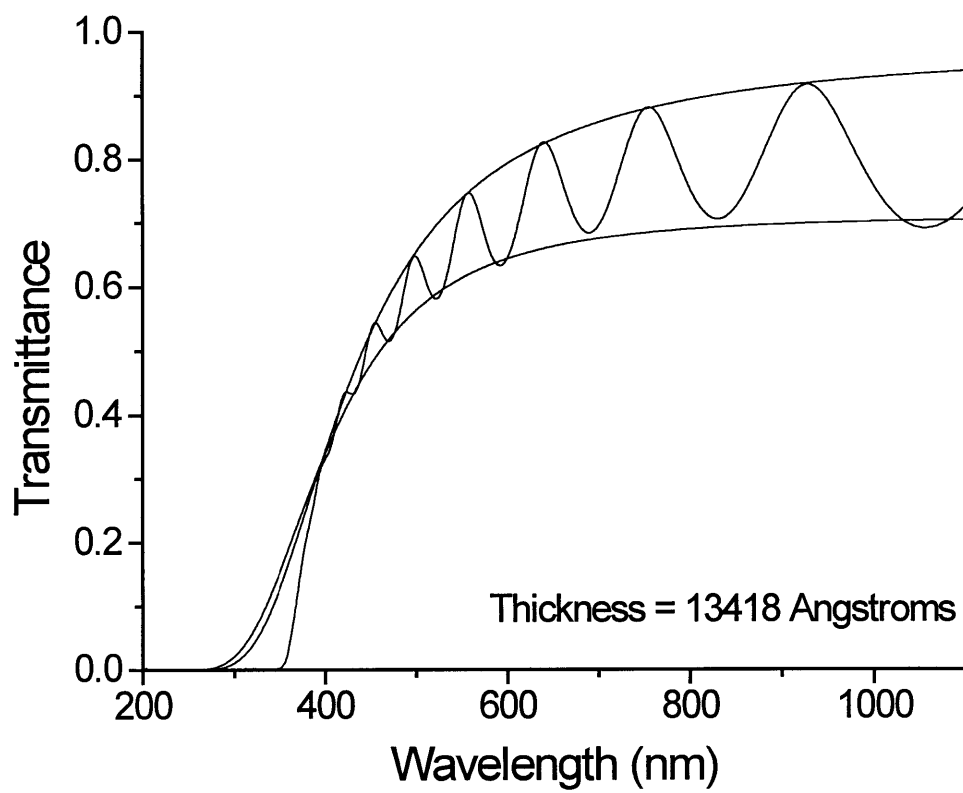


Figure 2.5. A typical UV/Vis transmission spectrum from a CeO₂ film on silica glass showing curve fits generated during calculation of film thickness.

non-uniformities in film thickness can significantly effect results, however. This method works only for films of thickness greater than approximately 1000 Å. It was necessary to grow thick films as controls, obtain correction factors for the as monitored thickness values from the rate monitor, and back calculate actual film thicknesses for the samples produced in this study since the thickness of most films deposited during this study was only 250 Å. All thicknesses reported are those read on the quartz crystal monitor, not the actual film thicknesses calculated from optical data.

Crystallographic orientation

Crystallographic orientation of the films was determined using X-ray diffraction. A 12kW Rigaku rotating anode X-ray generator and Rigaku diffractometer with a pole figure attachment were used to collect both $\theta/2\theta$ powder patterns and β scans.⁴³ $\theta/2\theta$ scans were collected at a fixed χ value of 90°. All beta scans were collected at $\chi=35^\circ$ from the plane of the substrate on the CeO₂ (111) peak at approximately 28.56° 2 θ , unless otherwise noted. See figure 2.6 for schematic diagrams of the x-ray experiments performed.

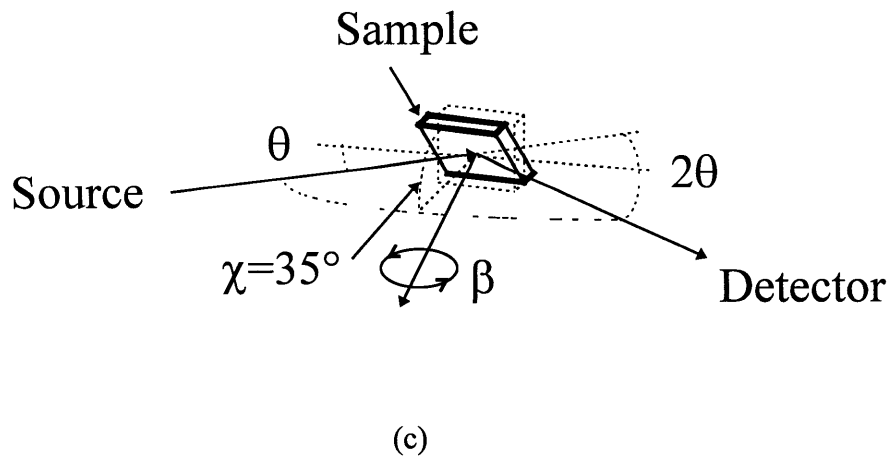
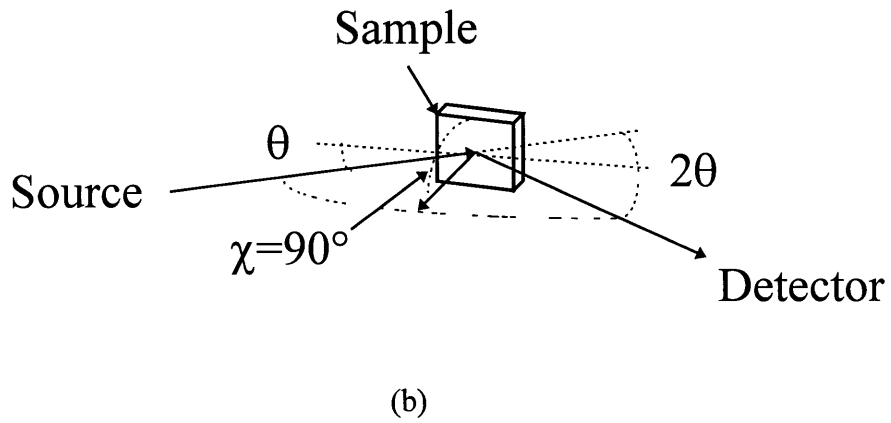
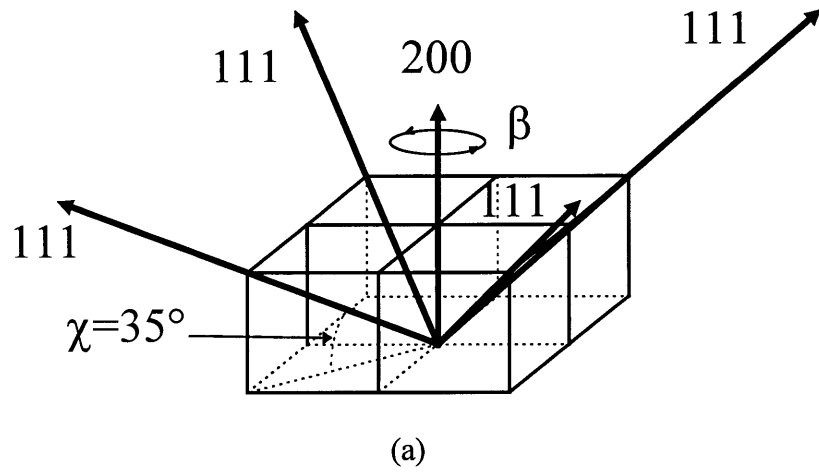


Figure 2.6. The arrangement of (200) and (111) poles in a cubic material such as CeO_2 or nickel is shown in (a). Shown in (b) and (c) are the experimental setups for $\theta/2\theta$ scans and β scans, respectively. The angles θ , 2θ , β , and χ are identified.

CHAPTER 3: RESULTS

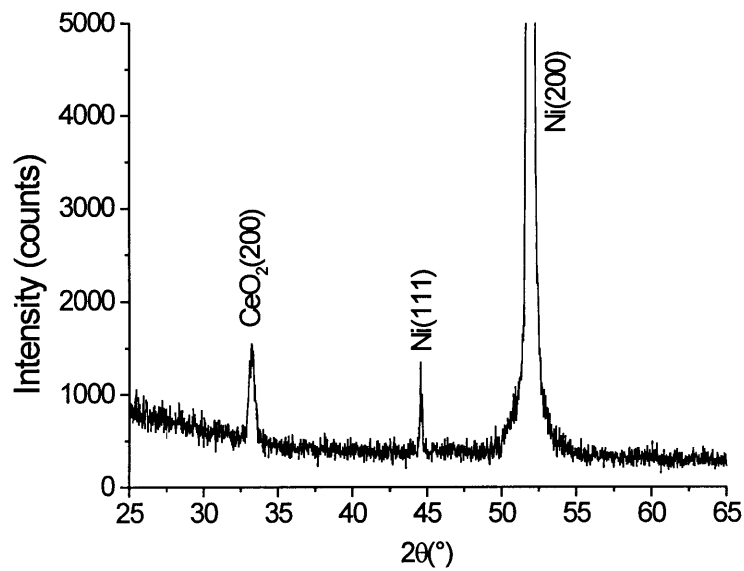
Crystallographic orientation

Deposition from cerium on nickel

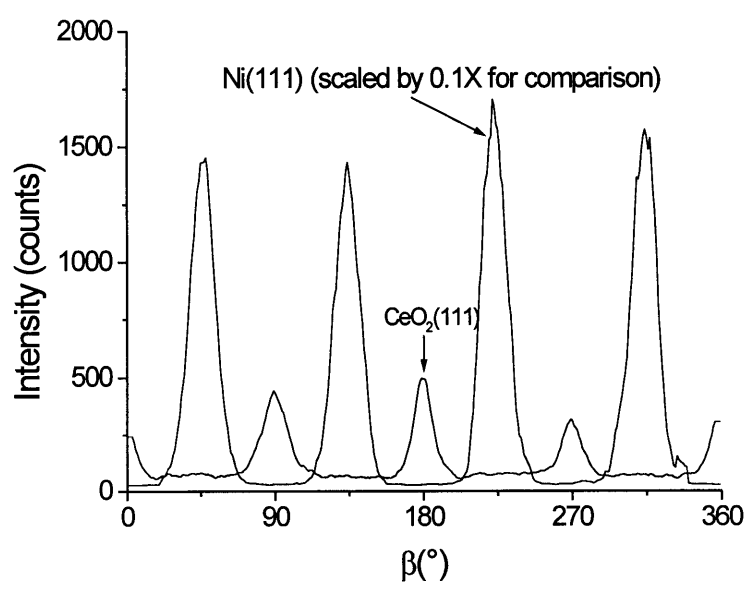
The diffraction patterns from a cerium source deposition on nickel are shown in figure 3.1. Deposition was carried out at 650°C. The deposition rate was 0.5 Å/s. The film was deposited in 1.0 sccm flowing forming gas, resulting in a deposition pressure of approximately 2.5×10^{-5} mm Hg. Total film thickness was 250 Å. Samples were heated to 650°C in approximately 1 mm Hg forming gas and held for 5 minutes to remove any NiO present on the substrate prior to deposition. There is only (200) oriented ceria present, as indicated by the $\theta/2\theta$ pattern in figure 3.1 (a). The film is epitaxial to the nickel substrate with a 45° rotation in the plane of the substrate, as shown in the beta scan of the CeO₂ (111) and Ni (111) poles depicted in figure 3.1 (b). The full width at half maximum (FWHM) for the CeO₂ film (~16°) is comparable to that of the underlying nickel substrate (~18°).

Deposition from oxide on nickel

Initial attempts to deposit CeO₂ from a CeO₂ source directly on nickel by electron beam evaporation were unsuccessful. Such depositions yielded (111) wire texture ceria with no in plane orientation, as indicated in figure 3.2 (a). Figure 3.2 (b) shows a 200 beta scan at $2\theta=33.08^\circ$, $\chi=35^\circ$ from the plane of the substrate. This film was deposited at 1.0 Å/s in an atmosphere of forming gas (Ar/5%H₂). The flow rate of the gas was 5.0 sccm.

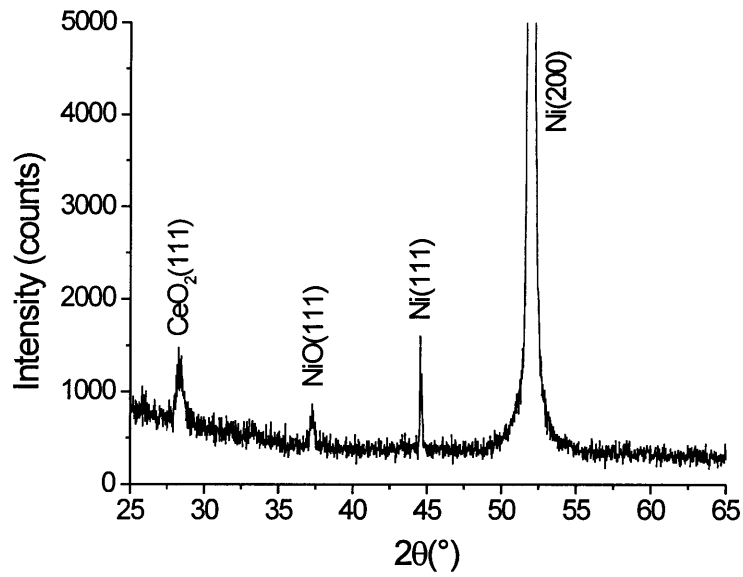


(a)

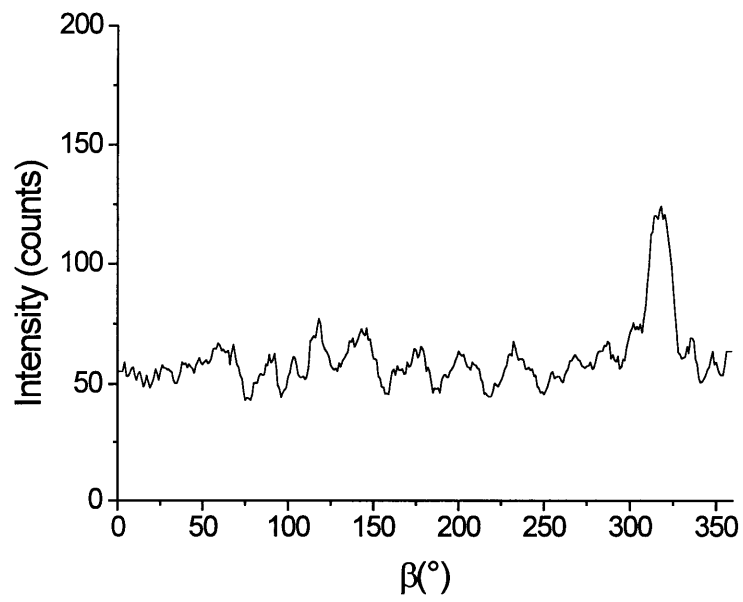


(b)

Figure 3.1. Diffraction patterns of a CeO_2 film deposited on nickel from a cerium metal source. A $\theta/2\theta$ pattern is shown in (a). The (111) β scans of the nickel substrate and epitaxial CeO_2 film are shown in (b).



(a)



(b)

Figure 3.2. $\theta/2\theta$ diffraction pattern for a CeO_2 film deposited on a nickel substrate from a CeO_2 source (a). Shown in (b) is the (200) β scan of the CeO_2 film.

Prior to deposition, the substrate was heated to 650°C in approximately 1 mm Hg forming gas for 5 minutes to remove any NiO scale present on the substrate. Such a purge was sufficient to produce epitaxial deposits of CeO₂ by reactive evaporation of cerium metal on nickel. Note, however, that NiO has formed on the substrate at some point during the deposition (as indicated by the $\theta/2\theta$ scan).

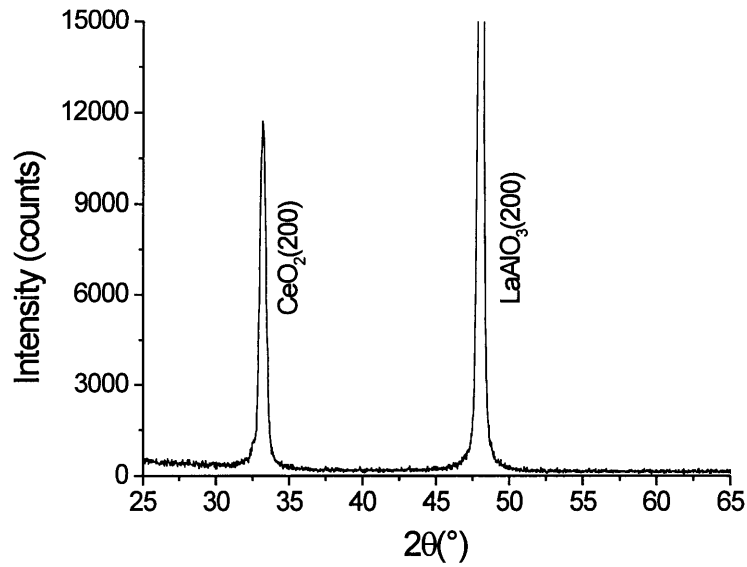
Deposition on oxides

Deposition of CeO₂ on LaAlO₃ substrates typically produced epitaxial films regardless of deposition source. Figures 3.3 and 3.4 show results from films deposited on LaAlO₃ substrates during the same depositions as described above (on nickel substrates). By comparing samples from the same deposition, any variation in chamber conditions from one run to the next is eliminated. As the X-ray scans indicate, films from both the cerium metal and CeO₂ source depositions were epitaxial to the single crystal LaAlO₃ substrates.

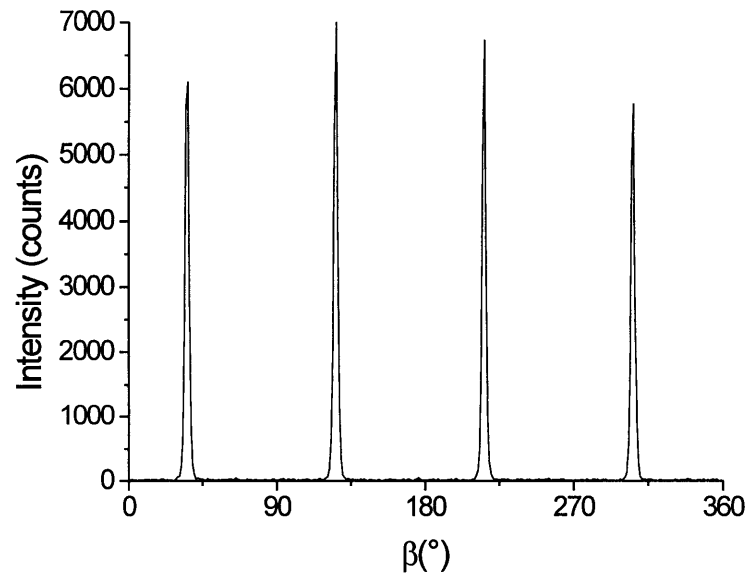
Reproducibility issues

Epitaxial Reproducibility

While nearly all CeO₂ source depositions demonstrated the same epitaxy, independent of process conditions, the cerium metal source depositions showed considerable variability from one run to the next. For example, three runs on single crystal nickel substrates, processed under the same temperature, deposition rate, and gas flow gave three completely different results, as indicated in figure 3.5. One film demonstrates (200) epitaxy, the second exhibits (111) wire texture, and the third cerium deposit appears to

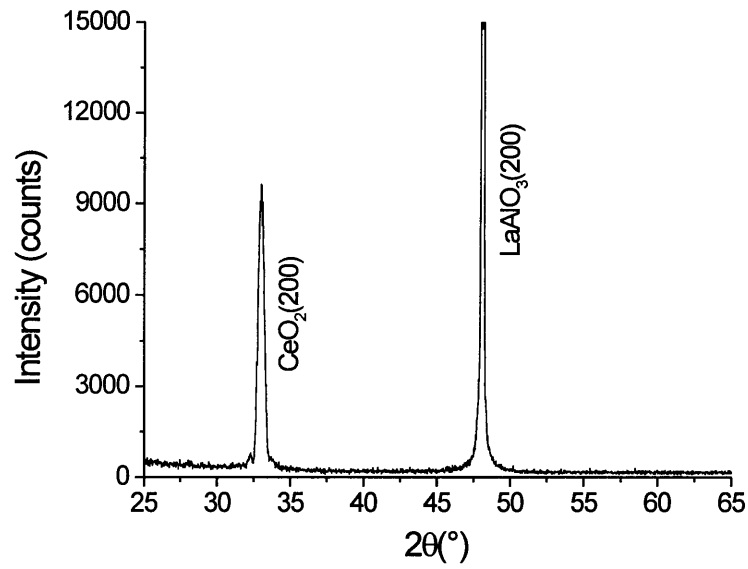


(a)

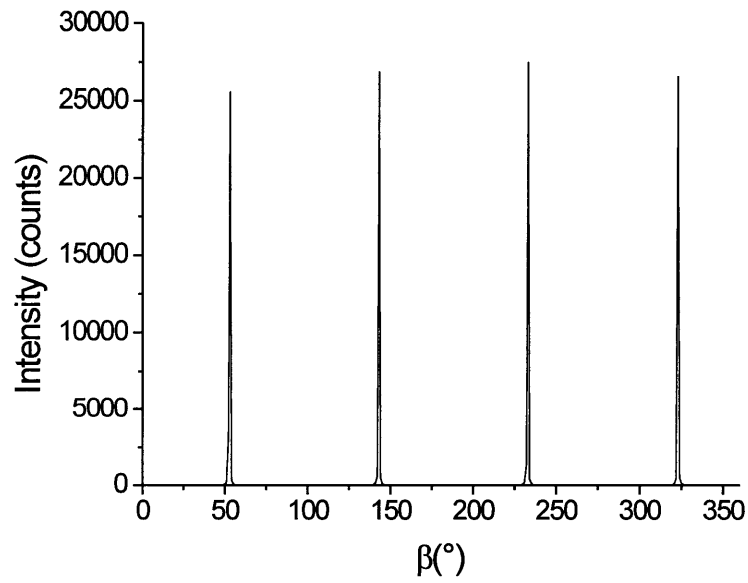


(b)

Figure 3.3. Diffraction patterns of a CeO_2 film deposited on LaAlO_3 from a cerium metal source. Depicted in (a) is a $\theta/2\theta$ scan, while (b) shows the (111) CeO_2 β scan.



(a)



(b)

Figure 3.4. Diffraction patterns of a CeO₂ film deposited on LaAlO₃ from a CeO₂ source. The $\theta/2\theta$ scan is shown in (a). The (111) CeO₂ β scan is shown in (b).

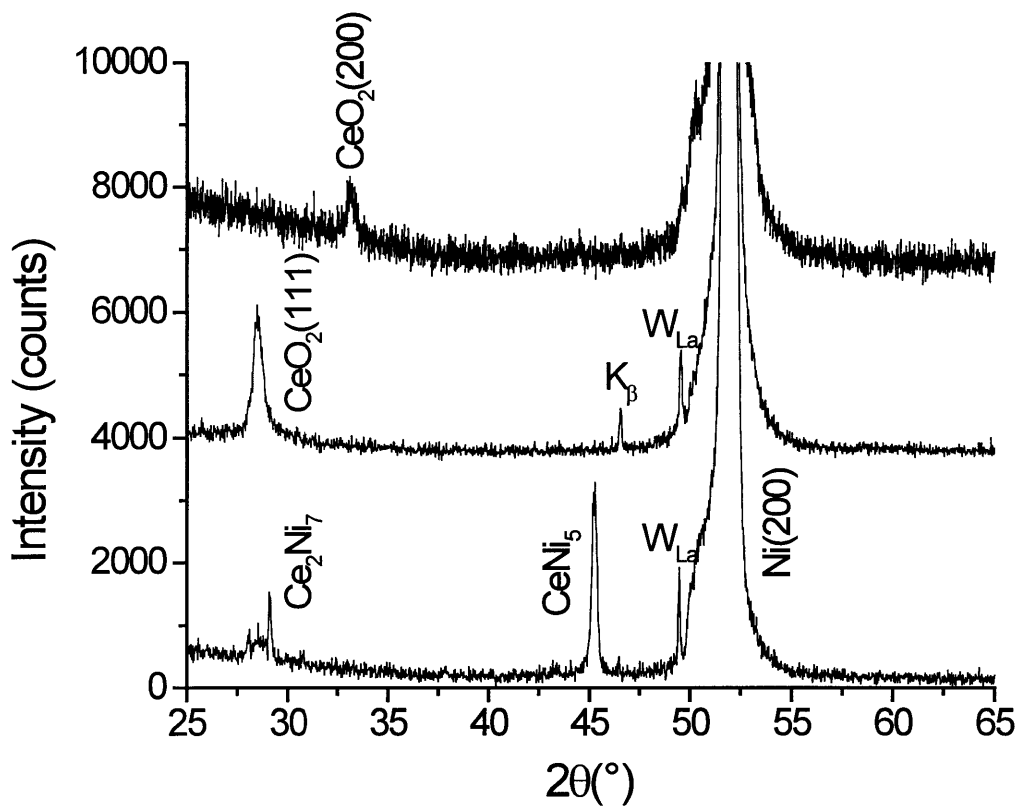


Figure 3.5 The $\theta/2\theta$ scans shown demonstrate the lack of reproducibility in CeO_2 films deposited by reactive evaporation of cerium metal on single crystal nickel substrates. All three films were processed under the same conditions (1 $\text{\AA}/\text{s}$, 650°C, 1-2 sccm Ar/5% H_2). The resulting films demonstrated (200) epitaxial alignment, (111) wire texture, and alloying of the cerium metal with the nickel substrate, respectively.

have alloyed with the substrate rather than reacting with ambient oxygen to form CeO_2 . A series of depositions designed to test the effect of oxygen content in the background gas composition during deposition revealed that the highest and lowest oxygen partial pressure depositions ($\text{Ar}/8\%\text{O}_2$ and $\text{Ar}/5\%\text{H}_2$, respectively) produced epitaxial films on LaAlO_3 , whereas a mix of the two gases ($0.7 \text{ sccm Ar}/5\%\text{H}_2 + 0.3 \text{ sccm Ar}/8\%\text{O}_2$) yielded a mixed (200)/(111) oriented CeO_2 film. These results are shown in figure 3.6. It is difficult to explain these results unless some critical process parameter is not well controlled from one deposition to the next.

Sources of variation

Parameters which can be controlled during a deposition include temperature, deposition rate, angle of incoming deposition flux relative to the substrate, background pressure and background gas composition. The reproducibility of deposition temperature, rate, and angle of incoming flux are all fixed within a rather small margin of error. The background pressure during deposition is fixed within an order of magnitude. Errors are introduced in that one set of gas correction values for the ionization gauge are used for the mix of gasses in the chamber (Ar , O_2 , H_2 , etc). A drift in the value read by the ion gauge has also been noticed after measuring pressure for an extended duration in forming gas, indicating some degradation of the gauge itself. Thus, the measured background pressure during deposition is subject to some variability. This should not effect the resulting film, however, since the same gas flows are used from one deposition to the next. The pressure that results when $1 \text{ sccm Ar}/5\%\text{H}_2$ is flowed into the system may not always read the same value, but the flow into the chamber is the same.

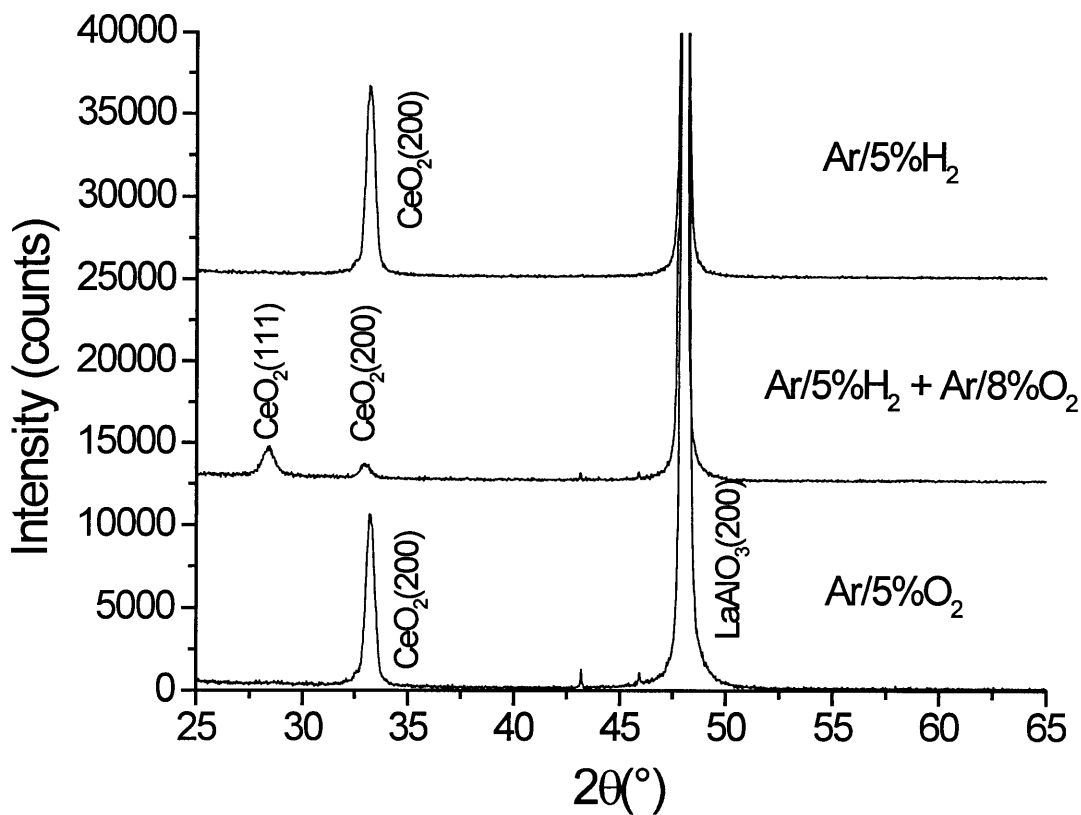


Figure 3.6. The $\theta/2\theta$ scans of CeO_2 films on $LaAlO_3$ substrates demonstrate a lack of reproducibility of epitaxy when depositing from a cerium metal source. Oxygen content of the background gas increases from the top scan to the bottom scan, yet only the film processed in a gas composition of intermediate oxygen partial pressure exhibits a polycrystalline component.

This leaves the gas composition in the chamber as a source of variability. The chamber used during these studies does not utilize a loadlock and is, therefore, vented to atmosphere every time a new sample is loaded. This provides ample opportunity for water vapor, oxygen, and other atmospheric contaminants to adsorb to the chamber walls. The chamber is then pumped down to a base pressure of at most 2.5×10^{-7} mm Hg before beginning a deposition. It is possible that the walls are still contaminated at this point. As the chamber walls are radiatively heated by the electron gun, these contaminants desorb into the chamber. The result is a gradual change in background gas composition during deposition.

Experimental evidence for the variation of background gas composition

Depositions to different thicknesses of material supported this notion. It was found that while thin films deposited at 650°C in a mix of 0.7 sccm Ar/5% H_2 and 0.3 sccm Ar/8% O_2 at 0.5 \AA/s from a cerium metal source were epitaxial to the underlying nickel substrate, the epitaxial relationship was lost as film thickness was increased. This effect is shown in figure 3.7. The same is not true of films deposited from a CeO_2 source. Figure 3.8 indicates that as film thickness deposited from a CeO_2 source increases, epitaxy is maintained. These depositions were performed at 600°C and 1.0 \AA/s in an ambient atmosphere (no gas flowing into the chamber). The result points to one of two conclusions. Either the change in background gas composition does not have the same effect on an oxide source deposition as it does on a metal source deposition, or the change in background gas composition itself is linked to the choice of source material. Multiple depositions from a cerium metal source were performed over extended periods without

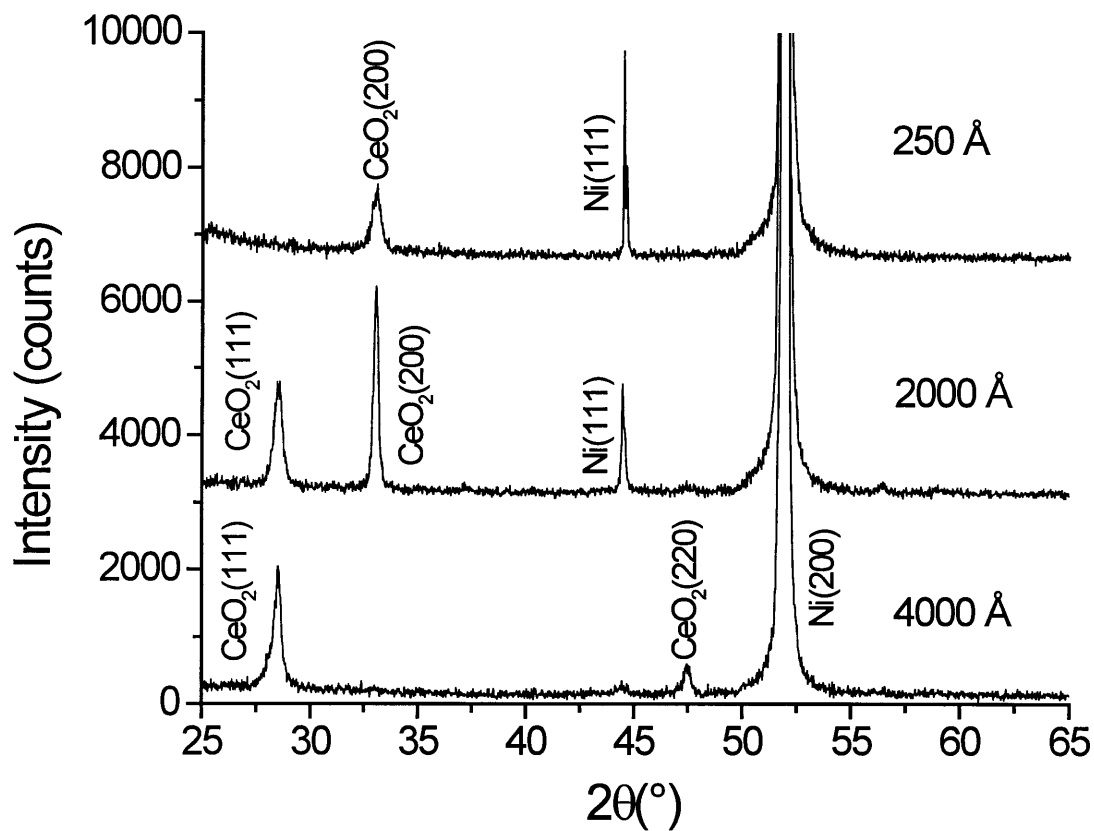


Figure 3.7. CeO₂ films deposited on nickel substrates from a cerium metal source undergo epitaxial growth at low film thickness, but lose this epitaxial relationship as film thickness increases, as indicated by X-ray $\theta/2\theta$ diffraction patterns.

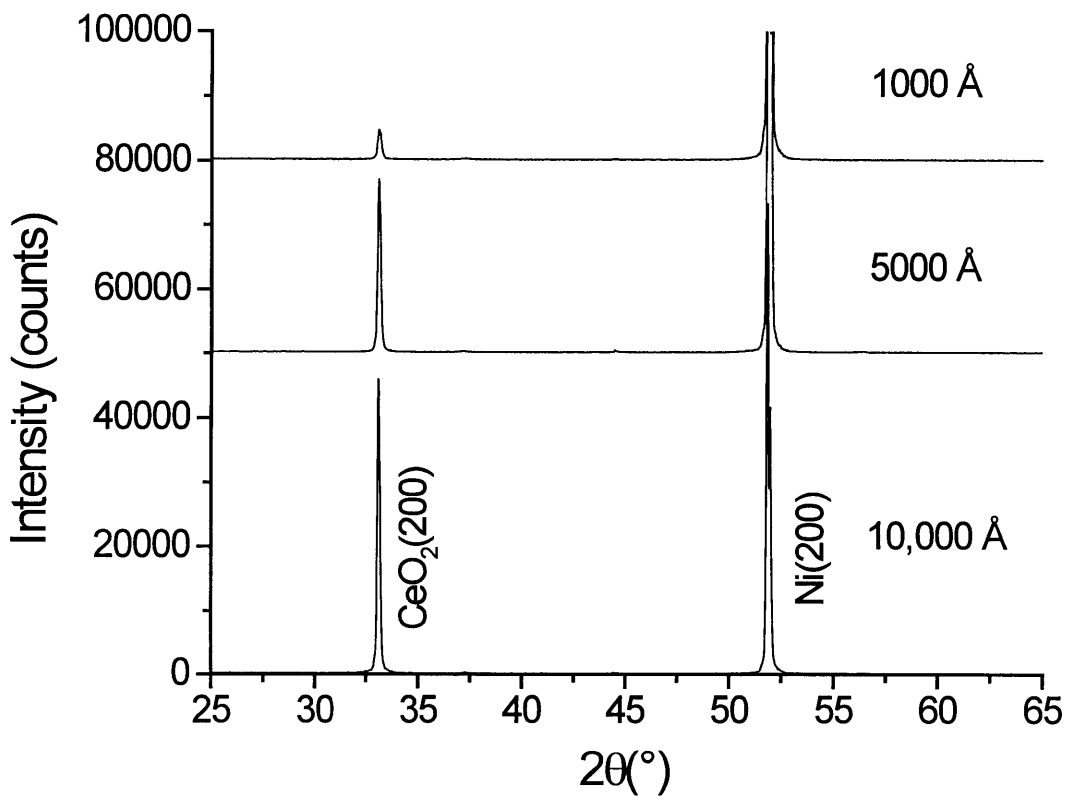


Figure 3.8. CeO₂ films deposited from a CeO₂ source maintain an epitaxial relationship to the substrate, independent of film thickness, as indicated by X-ray $\theta/2\theta$ patterns. The films were deposited on nickel substrates capped with a thin epitaxial layer of CeO₂ deposited from cerium metal.

venting the chamber in order to further investigate this apparent change of gas composition with time. A film was deposited as soon as the electron gun source had been conditioned, then the slot configuration sample shutter was closed but evaporation continued. A second substrate was exposed to the same deposition flux at a later time. The results of one such series are shown in figure 3.9. The first deposition produced epitaxial CeO_2 , whereas the second film, deposited after a total of three hours of evaporation, exhibited evidence of alloy formation between cerium and nickel. This is strong evidence that the gas composition in the chamber changes as deposition continues. There was initially sufficient oxygen present to oxidize the cerium source deposition flux and form cerium oxide. There was insufficient oxygen present in the background gas to produce CeO_2 after three hours of deposition from the cerium metal source. Cerium metal was the deposited species after three hours of deposition.

It is worth noting that deposition of a metallic species can be observed after a long period of time. The metallic species begins to mirror the surfaces of the chamber walls when there is no longer sufficient oxygen in the chamber to oxidize the cerium being deposited. This mirroring results in a marked change of the appearance of the inside of the chamber from a rather dull, light tone to dark, reflective surfaces.

Film thickness calculations

Actual film thicknesses were calculated using the method of Swanepoel described earlier. Optical thicknesses were calculated for films with monitor thickness values of 2500, 5000, 7500, and 10,000 Å. The range of interest for the films deposited in this study

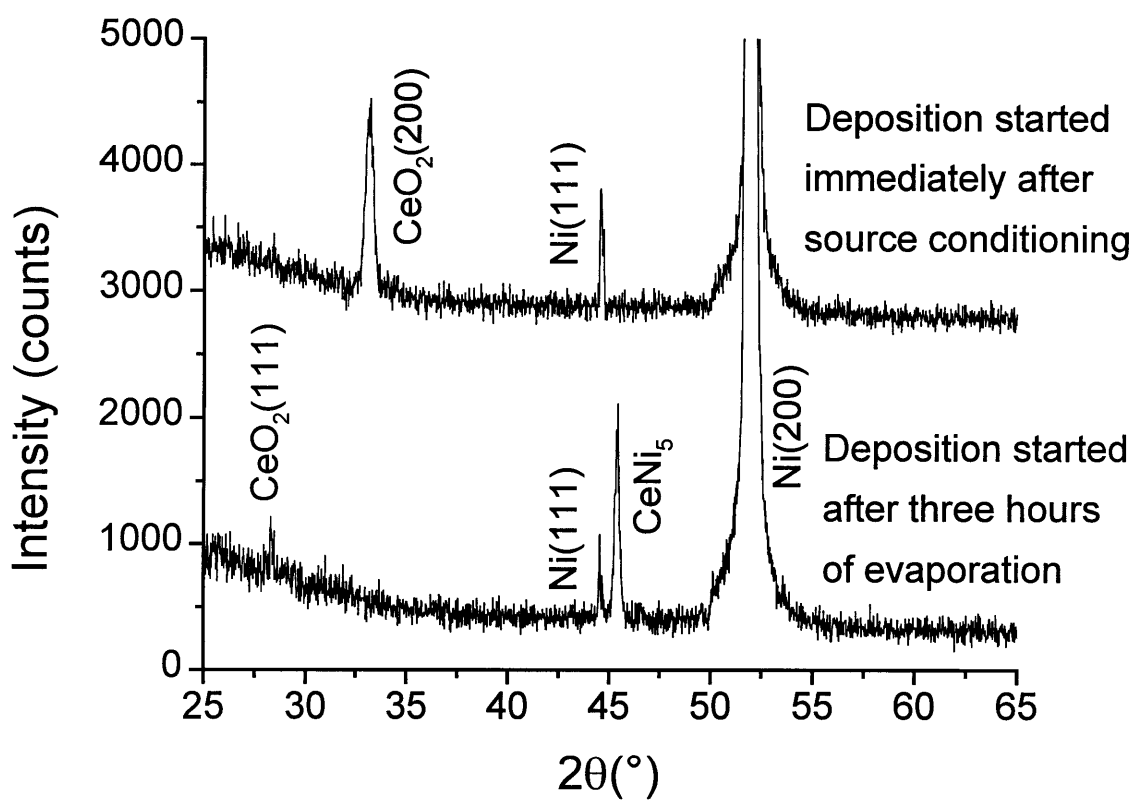


Figure 3.9. X-ray $\theta/2\theta$ patterns for two films deposited on nickel from a cerium metal source. The first film was deposited immediately after the cerium source was conditioned, while the second film was deposited after three hours of evaporation. The first film exhibits (200) epitaxial CeO₂, while the second shows evidence of alloying between the cerium metal and nickel substrate.

is outside the range for which Swanepoel's method is effective. It was necessary to extrapolate an approximate correction factor for the very thin (250 Å on the quartz crystal monitor) films deposited on nickel. The actual deposition rate when the monitor was set for 1.0 Å/s was approximately 0.91 Å/s, as indicated in figure 3.10.

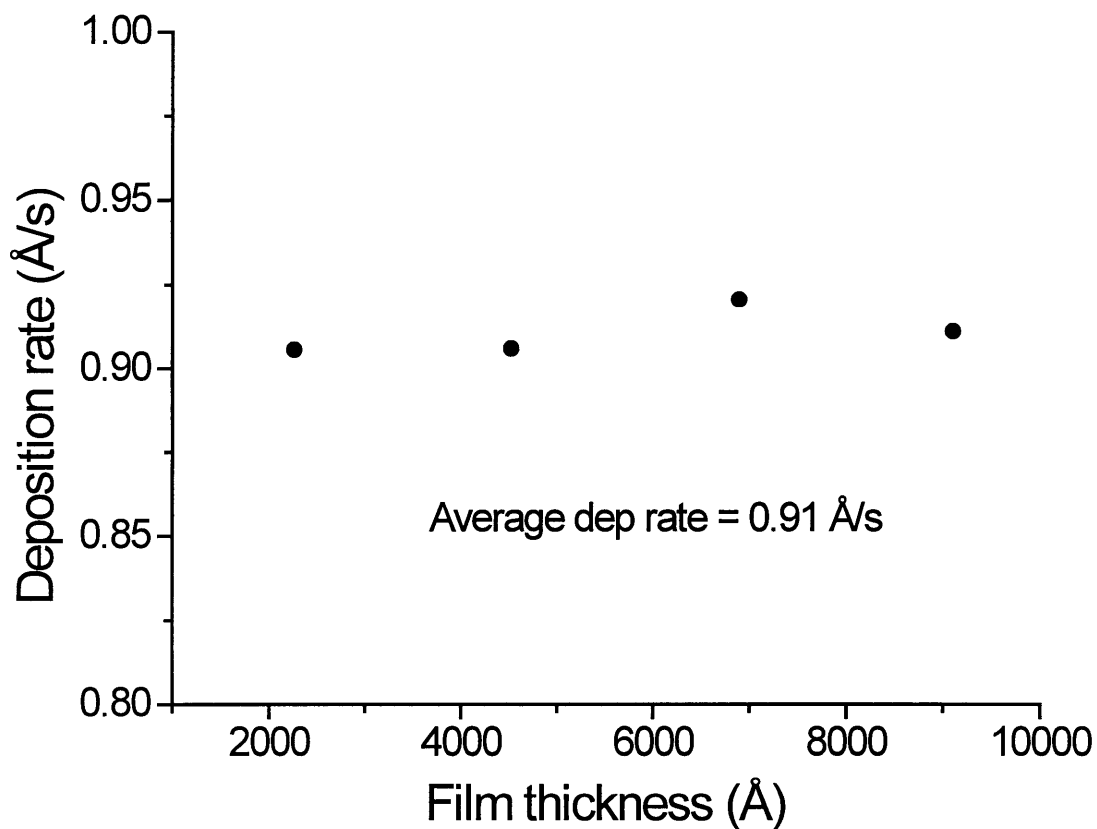


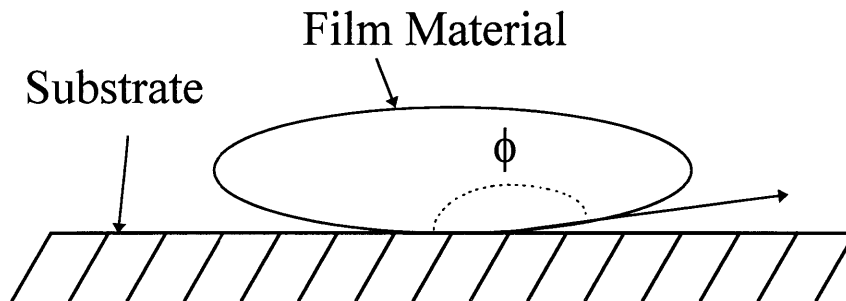
Figure 3.10. The figure shows average deposition rates for CeO_2 films deposited on silica glass substrates as calculated from optical thickness measurements as a function of total film thickness. The deposition rate programmed into the thickness monitor was 1.0 \AA/s , while the actual deposition rate achieved was 0.91 \AA/s .

CHAPTER 4: DISCUSSION AND TESTING OF MECHANISMS

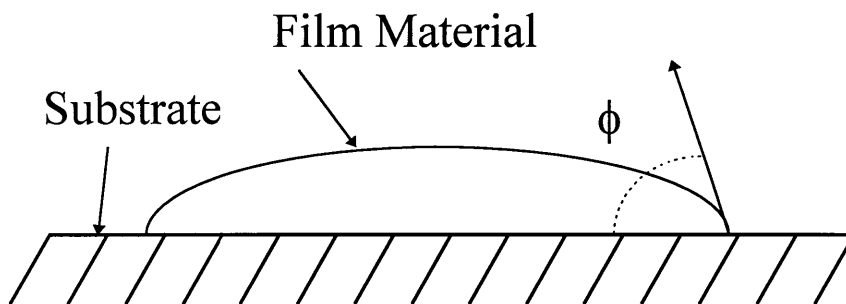
The empirical observation that epitaxial CeO_2 films can only be deposited on nickel from a metal source holds true despite the lack of reproducibility of films deposited on nickel from a cerium metal source. An explanation for this observation is required in order to gain insight to the processes occurring during deposition. Finding a solution to the reproducibility issues is very difficult without a mechanistic understanding of the deposition process.

Wetting angle mechanism

The differences from metal to oxide deposition source may be a simple result of differing wetting angles of the deposited species on the substrate. In general, the wetting angle of metals on oxides is high. If a film of oxide is deposited on a metal substrate where the wetting angle is high, the result will be a film which beads up and has a very small amount of surface area in contact with the substrate. Figure 4.1 (a) demonstrates such a case. As a result, the film will not deposit epitaxially, but will assume whatever the lowest energy configuration for the deposited species is, independent of the underlying substrate. Depositions on silica glass have shown that (111) oriented wire texture CeO_2 is the preferred orientation for a cerium metal deposition when no epitaxial relationship between the substrate and film exists. See figure 4.2. The likelihood of epitaxy is much higher if the wetting angle is reduced to the point where the deposited species is in intimate contact with the substrate, as shown in figure 4.1 (b). It is reasonable to assume that

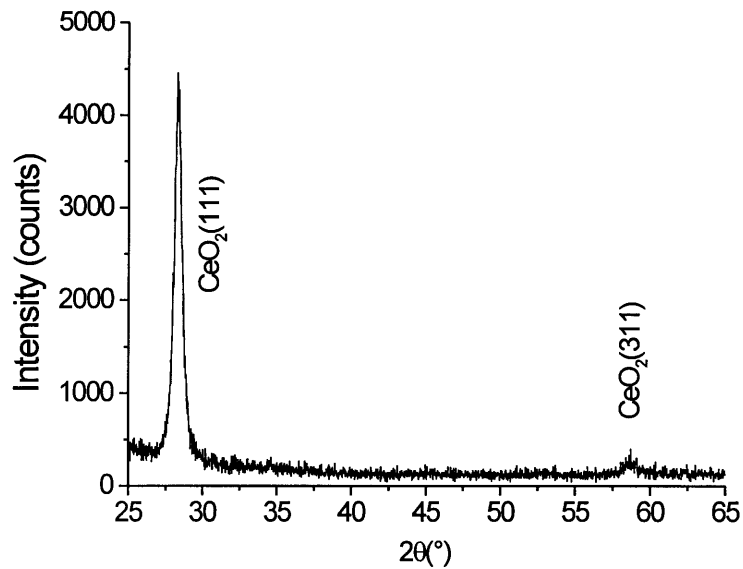


(a)

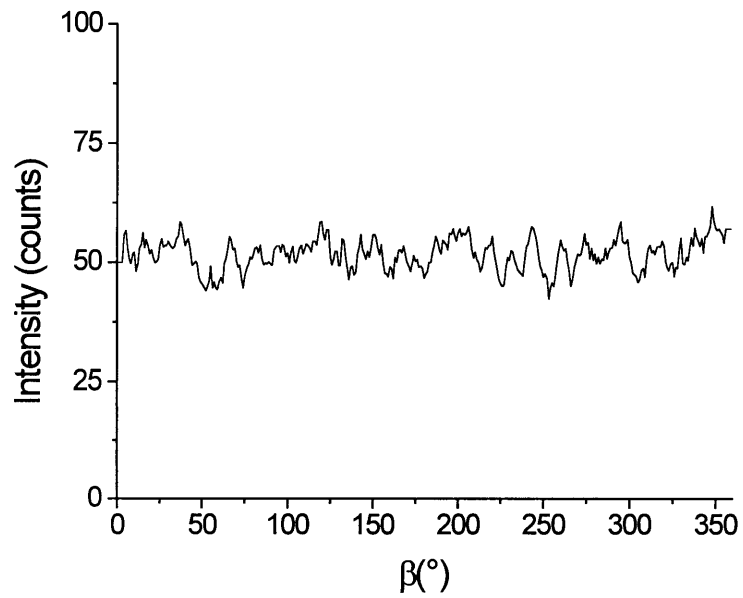


(b)

Figure 4.1. Surface contact area of a film deposited on a flat substrate varies as a function of the wetting angle (ϕ) of the deposited species on the substrate material. For high wetting angles, as depicted in (a), there is very little substrate contact, hindering epitaxial growth. For low wetting angles (b), substrate contact area is much higher, making epitaxial growth more probable.



(a)



(b)

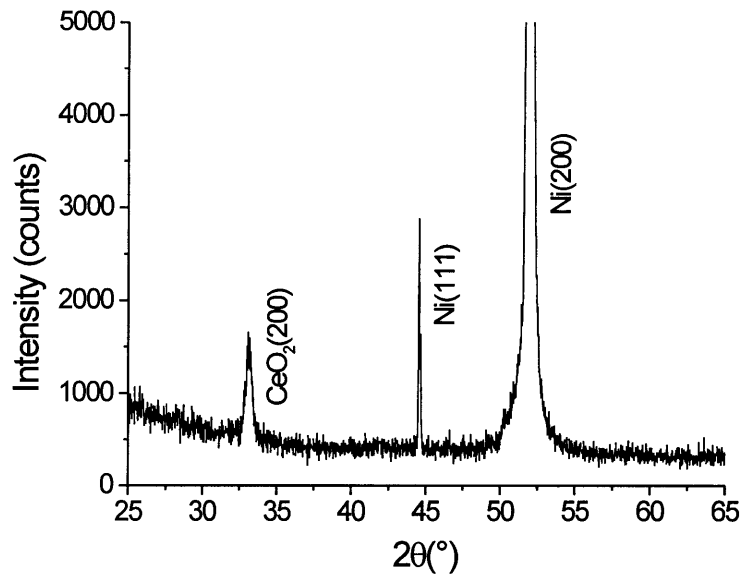
Figure 4.2. CeO_2 film deposited on a glass substrate by reactive evaporation of cerium metal. The favored alignment when no epitaxial relationship with the substrate exists is (111) wire texture, as indicated by the $\theta/2\theta$ scan (a) and (200) β scan (b) shown.

epitaxial deposition of a metallic species on a metallic substrate would be more likely than epitaxial deposition of an oxide species on a metallic substrate, since homogeneous systems (metal on metal) generally wet one another more easily than heterogeneous systems (oxide on metal).

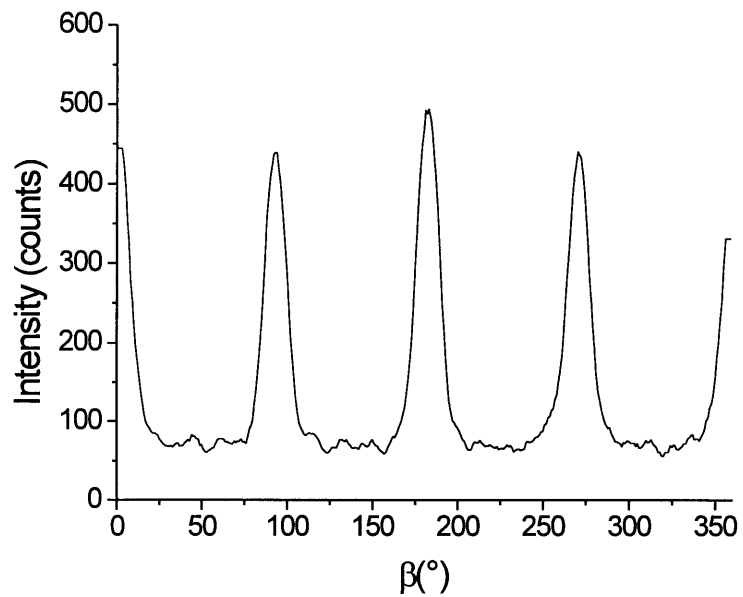
Reduced CeO₂ deposition

An attempt to significantly reduce the CeO₂ oxide source prior to deposition of a film on a nickel substrate was undertaken. The wetting angle theory suggests that if it were possible to reduce the CeO₂ to a metallic species, enhanced film/substrate contact would result, favoring epitaxial growth. The source was conditioned in forming gas to reduce it as much as possible prior to deposition. Substrates were covered with the sample shutter during this reduction step. Note that the oxide source darkens when heated under the electron beam, indicating an oxygen off-stoichiometry. Heating in a reducing atmosphere results in greater reduction of the source than heating in ambient. The electron gun crucible was rotated to cerium metal (without breaking vacuum) after reducing the oxide source material. The cerium source was then conditioned and used to getter any oxygen and/or water vapor from the chamber walls. Again, the substrates were covered during this conditioning. The crucible was rotated back to the CeO₂ source without breaking vacuum once metallic deposition from the cerium source was visually observed (as previously described), and a film was deposited from the reduced CeO₂ source on a deformation textured nickel substrate.

The results of the deposition described above are shown in figure 4.3. The film exhibits (200) biaxial alignment comparable to that of the substrate. The argument that



(a)



(b)

Figure 4.3. X-ray $\theta/2\theta$ and (111) β scans of a CeO_2 film deposited from a CeO_2 source on a nickel substrate ((a) and (b), respectively). The CeO_2 source was conditioned in forming gas, then excess oxygen in the chamber was removed using cerium metal as a getter prior to deposition from the pre-conditioned CeO_2 source. The diffraction data indicate that the film grew epitaxially on the nickel substrate.

wetting angle is controlling the epitaxy of the resulting film is supported, provided that the species deposited was actually a metallic species. It is necessary, however to verify that the species being deposited is metallic.

Thermodynamics of reduced CeO₂ deposition

Figure 4.4 shows an Ellingham diagram for the NiO and CeO₂ systems.^{44,45} According to this diagram, a P_{H_2}/P_{H_2O} ratio of 10^{14} would be required for metallic cerium to be the thermodynamically stable species during deposition at 650°C. Given that the forming gas flowing into the chamber consists of 5% H₂ and approximately 5 ppm impurities in the form of water or oxygen, the resulting P_{H_2}/P_{H_2O} ratio is approximately 10^4 , well below that required to stabilize the metallic species. It seems doubtful that reduction in forming gas could have provided a metallic species for deposition. Nonetheless, the values on the Ellingham diagram are equilibrium values, and it is possible that a non equilibrium phase reaches the substrate. The source itself is at extremely high temperature, potentially hot enough to allow reduction to a metallic phase. Experimental verification of the nature of the species being deposited is required.

Electrical characterization

A system was devised to obtain an order-of-magnitude estimate of the *in-situ* conductivity of the samples during deposition in order to experimentally test the nature of the species being deposited. Although off-stoichiometric cerium oxide conducts at high temperatures, the metallic conductivity of cerium metal is orders of magnitude higher than that of conductive ceria. This conductivity difference between metal and oxide was used to

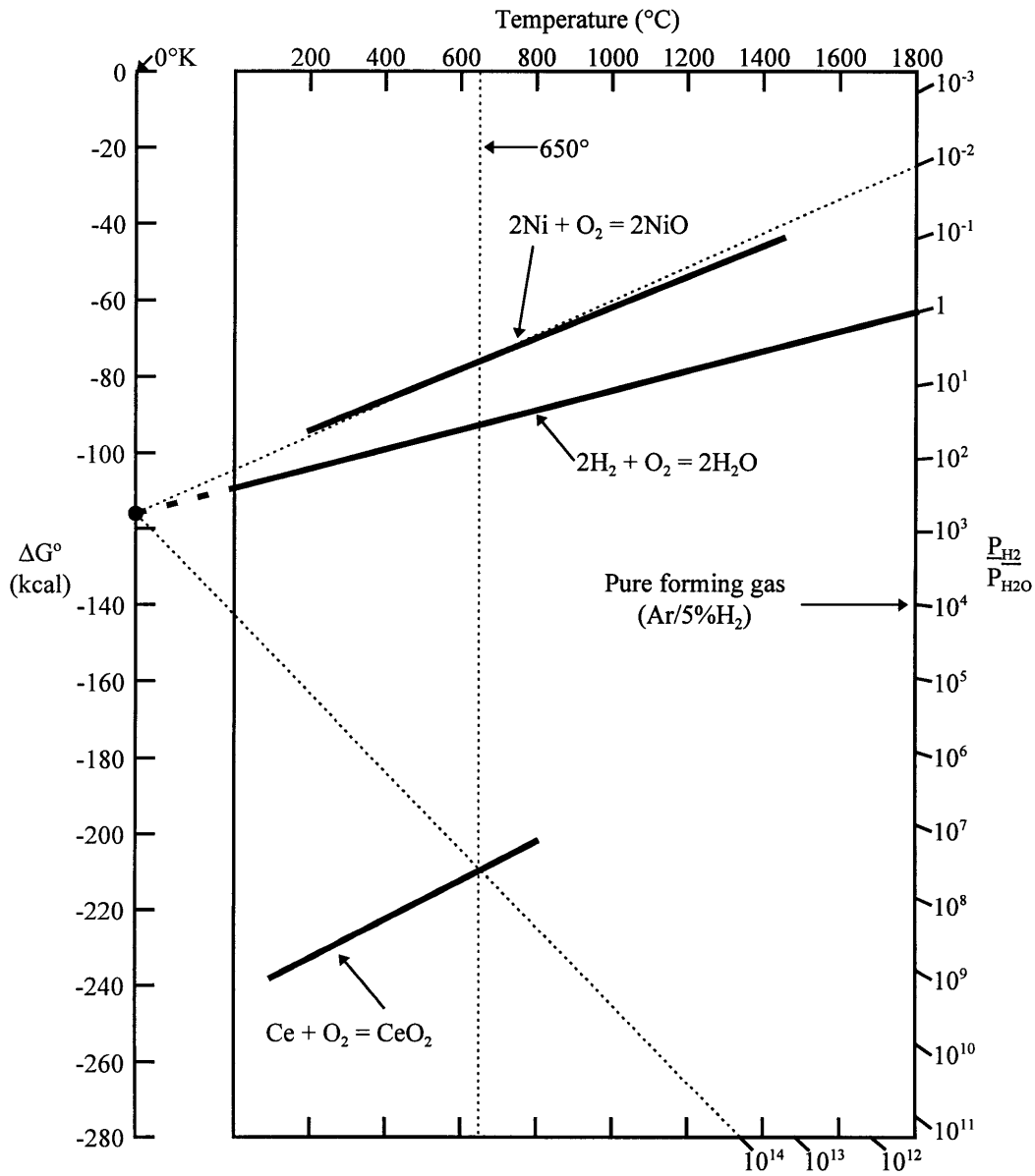


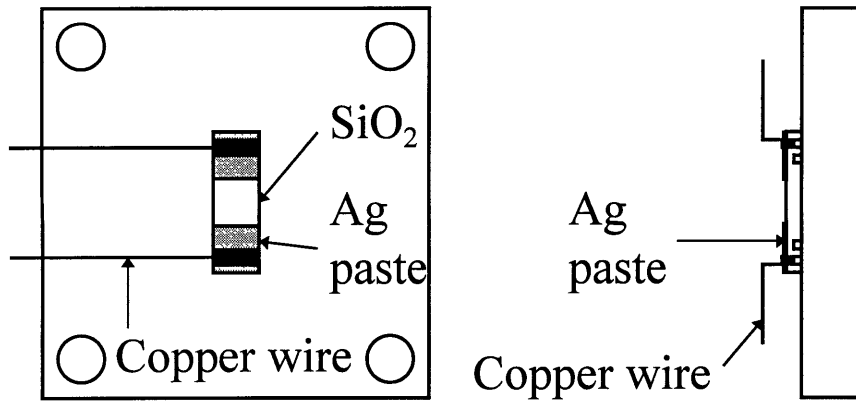
Figure 4.4. Ellingham diagram for NiO and CeO₂. The stability of these oxides as a function of temperature and gas composition may be read from the diagram.^{44,45}

determine whether or not the film deposited was metallic or an oxide of cerium (CeO, Ce₂O₃, CeO₂).

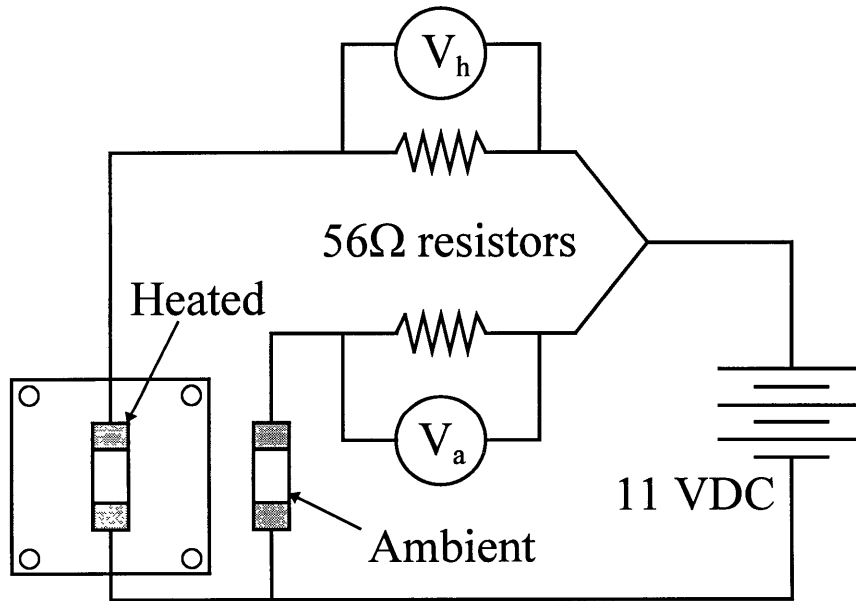
Experimental setup

Grooves were cut into silica glass substrates, allowing a fine copper wire to be attached to the ends of the substrate. Silver paste was then applied to this wire and an electrical contact pad was created at each end of the substrate. The substrate was then pasted to a stainless steel block as previously described. The wires were attached in such a way that the electrical contact pads were isolated from the sample mounting block. See figure 4.5 (a) for a diagram of the substrate setup used. A second substrate was suspended from the electrical contact wires approximately two inches from the substrate heater. This allowed concurrent collection and comparison of data from both a heated and non-heated sample.

The electrical response of the samples was measured using a circuit as diagrammed in figure 4.5 (b). A DC transformer was used as the power supply. Paper chart recorders served to measure the voltage drop across one of two 56Ω resistors in series with the heated and ambient samples, respectively. Voltage was measured across a resistor in series with the sample rather than across the sample itself so that prior to deposition the measured voltage would be zero. The voltage measured prior to deposition would have been the applied voltage had the voltage been measured across the samples, making detection of small voltage changes difficult. The applied voltage was approximately 11VDC, such that the current in the circuit was limited to <400mA if both samples shorted simultaneously.



(a)



(b)

Figure 4.5. A schematic of the substrate geometry (a) and electrical circuit (b) used to perform *in-situ* conductivity measurements of films during deposition.

Control depositions

Control depositions were performed in order to gauge the effectiveness of the *in-situ* conductivity setup prior to depositions under conditions of interest. A 1000Å thick film was deposited from cerium metal in 5 sccm forming gas after a long purge (metallic deposition). The voltage drop across the control resistors for both the sample heated to 650°C and for the ambient sample (approximately 200±20°C) are shown in figure 4.6. This voltage is directly proportional to the conductivity of the sample. Conductivity of the ambient sample increased as soon as the sample shutter was opened and deposition began. A nearly linear rise in conductivity for the sample was observed until deposition stopped, then the highly conductive film oxidized, as indicated by the abrupt drop in conductivity. The response is a combination of an increase in conduction due to increased film thickness and a decrease due to oxidation of the film material. The rise in conductivity is not perfectly linear with increased film thickness since the film partially oxidizes as deposition proceeds. CeO₂ and Ce₂O₃ are very stable species, and therefore will react with even minute amounts of oxygen from the background deposition gas. The heated sample exhibits a delay in response (the conductivity does not increase as soon as the shutter is opened). The film deposited on this heated substrate was more reactive than the ambient sample. The film may have reacted more readily with atmospheric oxygen or even with the silica substrate itself as a result. CeO₂ is considerably more stable than SiO₂, therefore, cerium metal is capable of reacting with oxygen from the silica substrate. The delay in response exhibited by the heated film is most likely a result of film oxidation during deposition, no matter the source of oxygen. Likewise, the maximum conductivity of the

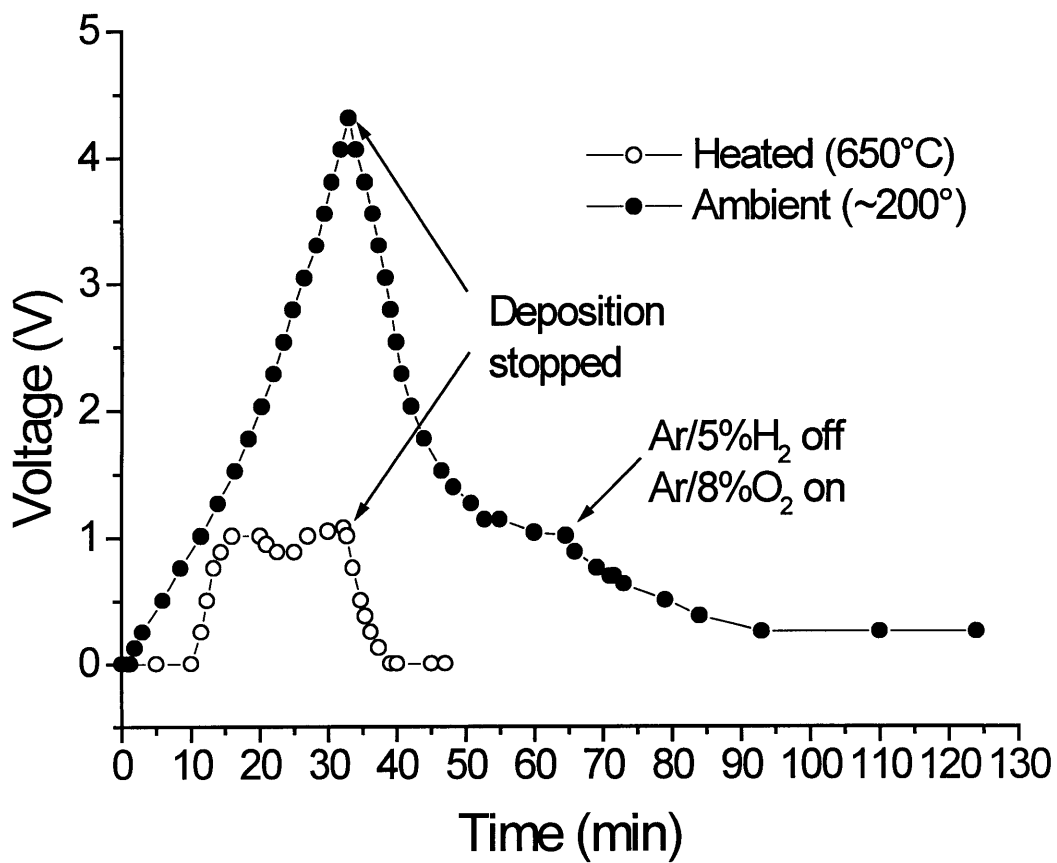


Figure 4.6. Voltage response of films deposited from cerium metal after a long cerium metal purge of the chamber. 1000Å of material was deposited in 5 sccm forming gas.

heated sample is less than that of the cold sample. Here, the increase in conductivity as a result of additional material deposition is balanced by the decrease due to oxidation of the film. Perhaps most importantly, note that the magnitude of the voltage response for these metallic depositions was on the order of a few volts. Figure 4.7 shows the electrical response of a 1000Å thick film deposited from a CeO₂ source in ambient atmosphere. During deposition, no change in conductivity is observed for either the heated or ambient sample. The material being deposited is an insulator. Prior to deposition, the sample was an open circuit, resulting in no voltage drop across the resistor. This did not change as material was deposited. Only when deposition stopped did the conductivity of the heated sample begin to rise. This indicates that while the film was being deposited, it was very close to being fully oxidized. The primary source of oxygen in the chamber (that is, oxygen evolved from the CeO₂ source itself) was removed when deposition was stopped, and the heated film began to reduce. The cold sample did not demonstrate this behavior since at 200°C, conductivity of the sample (whether it is reduced or not) is too low to observe. Appendix B shows a calculation of the amount of oxygen evolved from the source per unit time. A cosine distribution of evaporated flux from the source material is assumed. This allows calculation of the total amount of material evaporated into the chamber per unit time. The evaporant is assumed to undergo a reduction from stoichiometric CeO₂ to CeO_{1.9} upon evaporation from the source material. This liberates an equivalent flow of 0.13 sccm of pure O₂ into the chamber as a result of CeO₂ evaporation. This represents more than five times the flow of oxygen introduced to the background pressure during a reactive evaporation of cerium metal (0.30 sccm Ar/8%O₂).

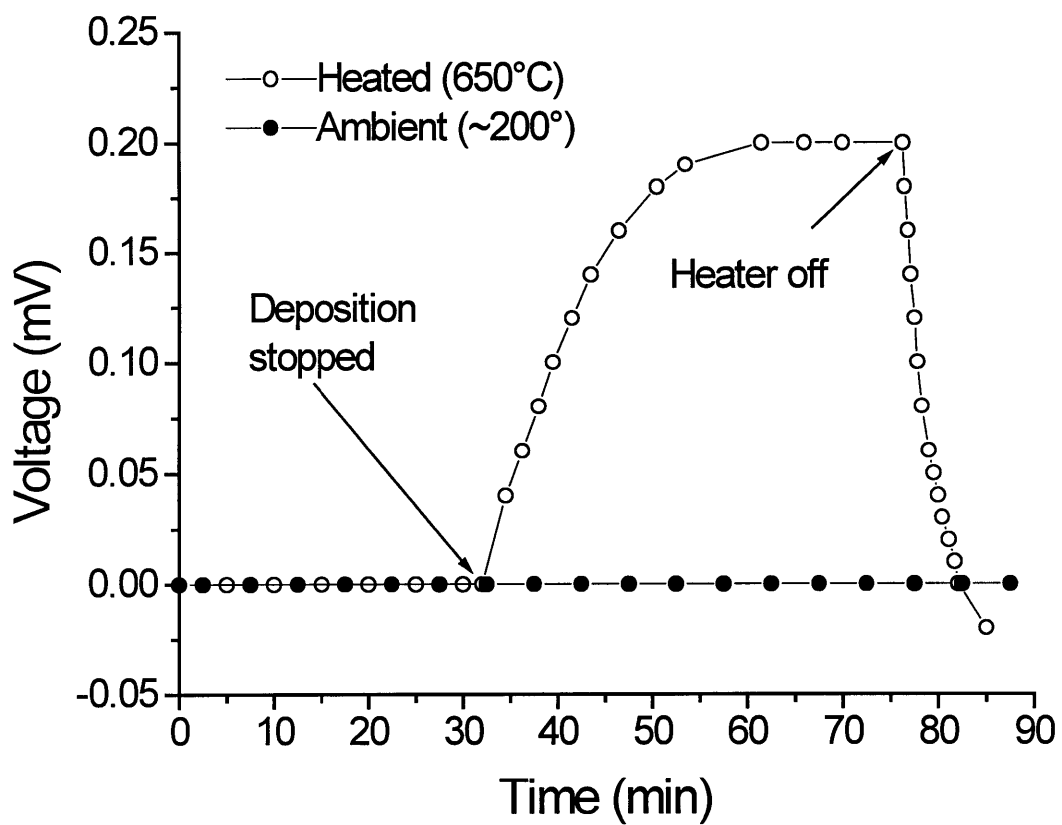


Figure 4.7. Voltage response of films deposited from CeO_2 in ambient atmosphere (no gas flowing).

Oxygen evolution from the source material is likely the most significant source of oxygen in the background chamber pressure during a CeO_2 evaporation. Note that when the run was complete and the hot sample was allowed to cool, its conductivity dropped to an unobservable level. Also, note that the magnitude of the response from this CeO_2 deposition was several orders of magnitude lower than the response demonstrated by a metallic film (less than 1 millivolt vs. several volts)

Electrical response during epitaxial depositions from cerium

Figure 4.8 shows the response of a film deposited from a cerium metal source in conditions which normally produce an epitaxial CeO_2 film on nickel. Total film thickness was 1000\AA , and the background gas composition was 0.7 sccm Ar/5% H_2 + 0.3 sccm Ar/8% O_2 . Here, a reduced species was deposited, as indicated by the immediate increase in conductivity observed when deposition started. Note that the cold sample showed no response, despite the fact that the response of the hot sample indicates that a reduced species was deposited. This is again due to the fact that at low temperatures, the conductivity of CeO_2 (whether reduced or not) is too small to observe. The incoming flux of reduced material was halted when deposition was stopped by closing the sample shutter. An abrupt decrease in the conductivity of the film was observed as the film oxidized. Another drop in conductivity is evident corresponding to the time the electron gun was shut off. Cerium vapor serves to getter any oxygen from the system. When the electron gun was shut off, the atmosphere in the chamber became more oxidizing. The film began to oxidize at a higher rate, resulting in a decrease in conductivity. The final drop in conductivity corresponds to the cooling of the sample. Note that the magnitude of the

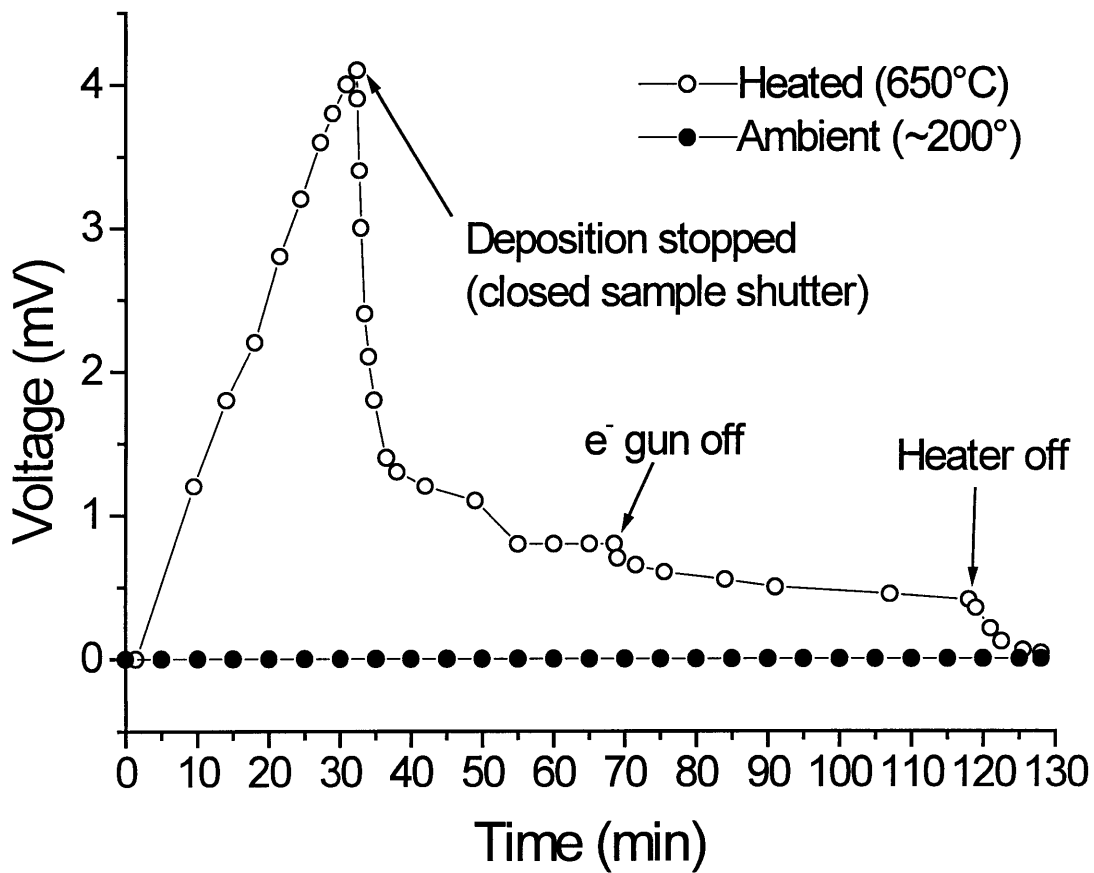


Figure 4.8. Voltage response of films deposited from cerium metal in a background gas composition consisting of 0.7 sccm Ar/5% H_2 + 0.3 sccm Ar/8% O_2 .

voltage response is on the order of a few millivolts. This corresponds to deposition of a reduced insulator, not a metallic deposition.

Electrical response during deposition from reduced CeO₂

In order to experimentally determine the nature of the species deposited during the run in which epitaxial CeO₂ was deposited from CeO₂ on nickel (in which the CeO₂ source was conditioned in forming gas, residual oxygen gettered from the chamber using the cerium metal source, then a film was deposited from the CeO₂ source), the run was repeated on an electroded silica sample. Figure 4.9 shows the voltage response for this run. During deposition, the voltage response was essentially constant. When deposition was stopped, the conductivity of the film increased. This behavior is characteristic of deposition of an oxide species. When deposition was stopped, the film was reduced. This is not possible if the film deposited was metallic. Also note that the magnitude of the voltage response is only a few tenths of a millivolt, indicative of an oxide species. The observed drop in conductivity prior to turning off the sample heater may be attributed to the cerium metal gettering step. During this step, the chamber walls were coated with cerium metal. This metal continued to absorb oxygen even once the CeO₂ deposition had begun. Once all cerium metal on the chamber walls reacted, the oxygen level in the background atmosphere increased and the film conductivity decreased as the film oxidized. With this evidence, the wetting angle theory may be discarded, since an epitaxial film has been deposited on nickel from an oxide species. If the wetting angle theory were valid, this oxide deposition would have beaded up on the surface of the substrate and produced a (111) wire texture or random polycrystalline film.

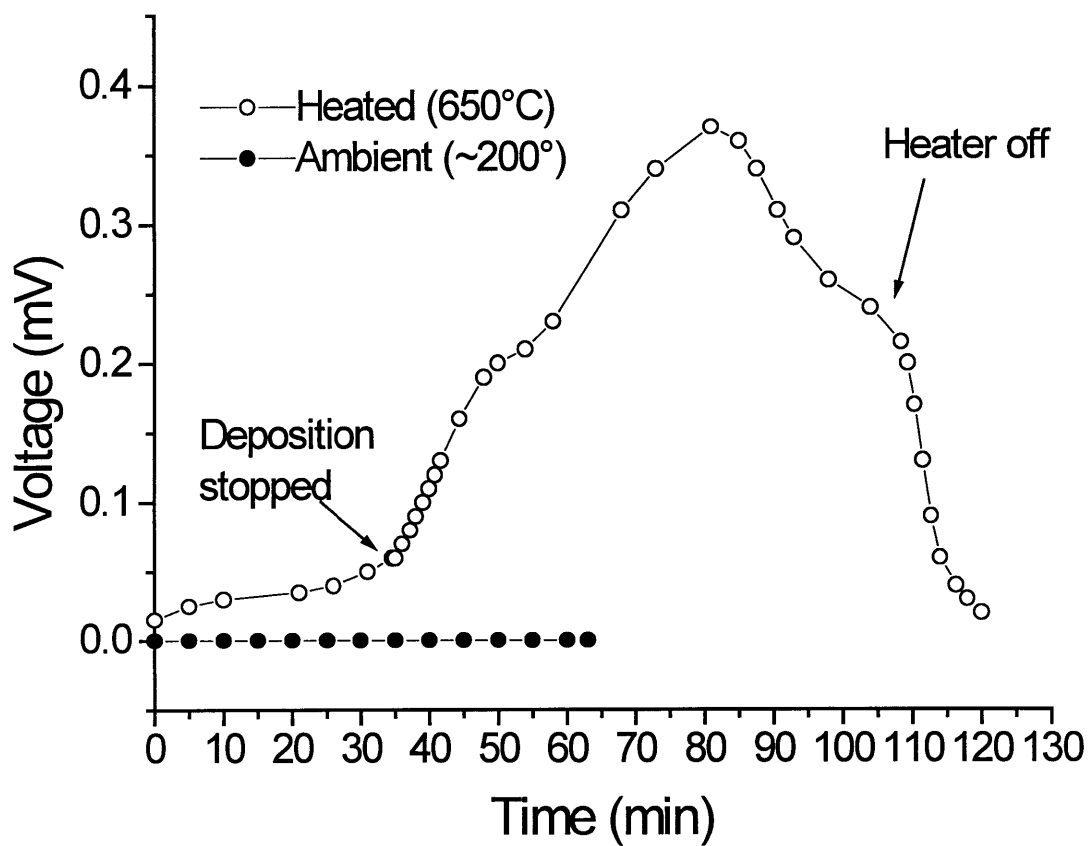


Figure 4.9. Voltage response of films deposited from CeO_2 after conditioning the CeO_2 source in forming gas and removing residual oxygen from the chamber using cerium metal as a getter.

Substrate contamination mechanism

The species deposited does not seem to be the controlling factor in determining the orientation of a CeO₂ film deposited onto a nickel substrate. Films deposited from CeO₂ in a forming gas ambient do not generally yield an epitaxial film, but when precautions are taken to reduce the background oxygen level, epitaxial film is deposited. Electrical behavior of films deposited in high or low background oxygen levels indicate that the same species of material is being deposited in each case. Since the deposition flux composition does not seem to be the controlling factor, the condition of the substrate must be questioned.

Thermodynamics of nickel oxide formation/reduction

According to the Ellingham diagram shown in figure 4.4, nickel oxide should be unstable in forming gas. The critical $P_{\text{H}_2}/P_{\text{H}_2\text{O}}$ ratio for NiO formation is approximately 10^{-2} for all temperatures. The Ar/5%H₂ forming gas used during these experiments has a $P_{\text{H}_2}/P_{\text{H}_2\text{O}}$ ratio of approximately 10^4 , more than sufficient to make the formation of nickel oxide thermodynamically unfavorable. It is possible that the background forming gas atmosphere is contaminated with oxygen from degassing from the chamber walls or, in the case of CeO₂ evaporation, from oxygen evolution from the source. If that contamination level is high enough, NiO formation on the substrate may be favored prior to deposition. When cerium metal is used as a source, the source serves as a getter to reduce this excess P_{O_2} in the chamber to a level where NiO is unstable, preventing oxide formation. If any oxide remains on the surface of the substrate, the highly reduced CeO₂ species deposited

from the cerium metal source may clean the surface of the substrate during the first few Angstroms of deposition as well.

Depositions from CeO₂ after purging with forming gas

Depositions were performed before and after long purges of forming gas in order to allow time to further degas the walls of the chamber prior to deposition. A film was deposited in flowing forming gas, then the electron gun was shut off, and the substrates were allowed to sit at temperature in an atmosphere of flowing forming gas for some length of time. A second film was then deposited on a second substrate (covered during deposition of the first film). Figure 4.10 shows the X-ray results of two films deposited in 1 sccm Ar/5%H₂ at 0.5 Å/s. The first film was deposited prior to a 6 hour purge in which 12 sccm Ar/5%H₂ was introduced into the vacuum chamber, resulting in a pressure of approximately 3×10^{-4} mm Hg. The second film was deposited after this forming gas purge. Neither film exhibits (200) epitaxial film. The run was repeated with a higher flow of forming gas during depositions (5 sccm), a higher deposition rate (1.0 Å/s), and a 12 hour purge during which the high vacuum valve to the chamber was closed. Chamber pressure increased to approximately 160 mm Hg during the 12 hour purge. The results of films deposited before and after the purge are shown in figure 4.11. The first film is primarily (111) oriented, while the second is primarily epitaxial to the substrate.

Oxygen evolution from the source

It is likely that sufficient oxygen is evolved by the source during conditioning to offset the $P_{\text{H}_2}/P_{\text{H}_2\text{O}}$ ratio of the background gas to the point where NiO is stable. Following the same model used to calculate the oxygen evolution from the CeO₂ source during

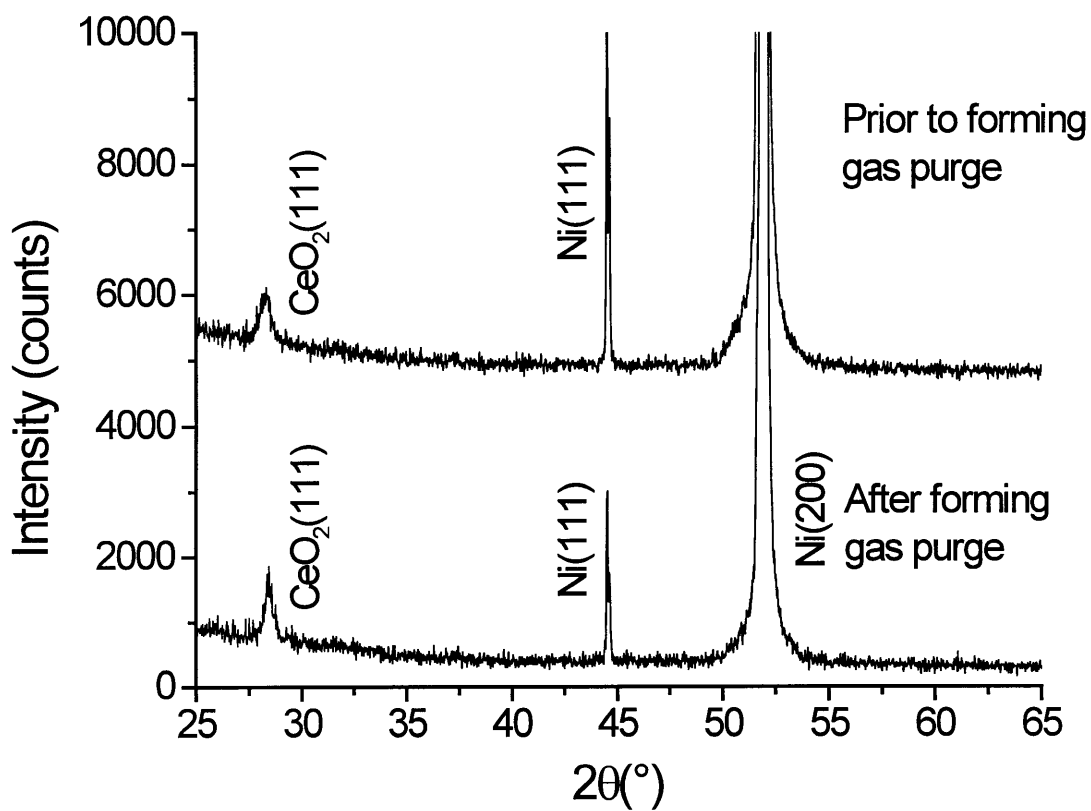


Figure 4.10. X-ray $\theta/2\theta$ scans of films deposited on nickel from CeO_2 before and after purging the chamber with 12 sccm forming gas for 6 hours (pressure during purge $\sim 3 \times 10^{-4}$ mm Hg). Films were deposited in a background of 1 sccm forming gas.

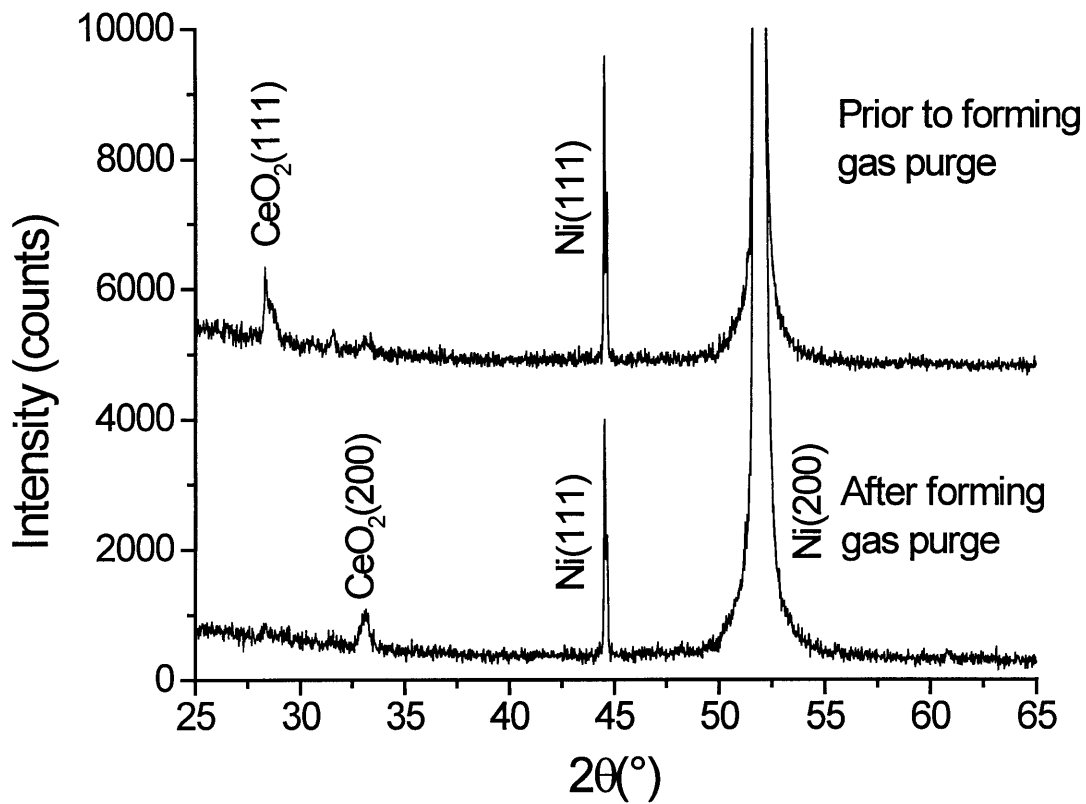


Figure 4.11. X-ray $\theta/2\theta$ scans of films deposited from CeO_2 before and after purging the chamber with 12 sccm forming gas for 12 hours. The chamber was not pumped during this purge, resulting in a rise of background pressure to approximately 160 mm Hg. Films were deposited in a background of 5 sccm forming gas.

deposition, a calculation was undertaken to determine the necessary stoichiometric change to result in NiO formation on the substrate prior to deposition. The calculation in Appendix C indicates that if the material evaporated is reduced from CeO_2 to $\text{CeO}_{1.96}$ during conditioning at 0.5 \AA/s in 1 sccm flowing forming gas, there will be sufficient oxygen introduced into the chamber atmosphere to stabilize nickel oxide before deposition begins. This oxide layer would in turn make epitaxial deposition impossible on the nickel surface. The fluorite structure is stable in CeO_x for compositions where x is as low as 1.72, so sufficient oxygen could be evolved from the source material and still leave sufficient oxygen for deposition of epitaxial CeO_2 .^{46,47} Also shown in Appendix C is a calculation indicating that the minimum flow rate of forming gas necessary to prevent NiO formation if the source does reduce from CeO_2 to $\text{CeO}_{1.72}$ upon evaporation is 14.1 sccm Ar/5% H_2 at a deposition rate of 0.91 \AA/s , higher than any flow rate used during a typical deposition.

There are several sources of error in these calculations. The CeO_2 is typically reduced when deposition starts. This means that upon conditioning, it will be reduced from some reduced CeO_{2-x} species to another CeO_{2-x-y} species. Large amounts of oxygen are evolved from the bulk source material at the beginning of deposition. The calculations assume that only material which is evaporated contributes oxygen to the background atmosphere, while in reality the bulk source itself contributes significant oxygen upon heating. No chamber leaks, backstreaming, or desorption of oxygen containing contaminants from the walls of the chamber are accounted for. All oxygen is assumed to exist as water. It is likely that some hydrogen/oxygen/water mix makes up the gas composition, rather than hydrogen and water alone. The approximation that the plume of

material coming from the source follows a cosine distribution is probably not accurate.

The calculation does, however, indicate that oxidation of the nickel substrate as a result of oxygen evolution from the source prior to deposition is a feasible explanation for the observed results.

Description of active mechanisms

The theory described above is consistent with all results presented. CeO_2 cannot, in general, be deposited on a nickel substrate by electron beam evaporation from a CeO_2 source since the conditioning of the source material introduces sufficient oxygen into the chamber to stabilize the formation of NiO on the surface of the substrate, destroying the epitaxial surface prior to oxide deposition. If care is taken to prevent this rise in oxygen partial pressure, the deposition of CeO_2 from a CeO_2 source is possible. The beginnings of epitaxy were observed when a sufficient amount of forming gas was introduced into the chamber to prevent NiO formation. The epitaxy obtained was as good as that obtained using a metal source when a cerium purge was used. The cerium metal purge prior to deposition both gettered any oxygen impurities from the chamber and coated the chamber with a layer of cerium metal. This metal continued to getter oxygen as the CeO_2 source was conditioned for deposition, preventing the nickel surface from oxidizing.

Reactive evaporation from a cerium source in a low P_{O_2} atmosphere on a nickel substrate is possible, but the oxygen level in the chamber must be both high enough so that the cerium deposited oxidizes prior to hitting the substrate, but low enough so that the formation of nickel oxide is thermodynamically unfavorable. If the oxygen level is too

low, cerium metal deposits onto the nickel substrate and forms an alloy, rather than epitaxial CeO₂. A calculation of the minimum oxygen flow necessary to oxidize all evaporated cerium to CeO₂ is shown in Appendix D. The assumptions involved in this calculation are much the same as previous calculations. The actual deposition rate of cerium metal from the source during deposition has not been accurately determined. It is not possible to measure the thickness of a cerium metal film or a highly reduced CeO₂ film using optical transmission data since the film material is generally quite opaque. The quartz crystal monitor parameters used during cerium metal deposition were identical to those used for CeO₂ deposition. For the purposes of the calculation, a maximum deposition rate of 0.1 Å/s is assumed when the rate monitor is set to 0.5 Å/s (using CeO₂ film parameters). The calculation indicates that during a typical reactive evaporation, more than ten times the amount of oxygen provided by the 0.3 sccm Ar/8%O₂ introduced during this study may be required to avoid metallic deposition onto the substrate and subsequent alloy formation. A flow of 10.5 sccm Ar/5%H₂ would also have to be introduced to prevent formation of NiO prior to deposition. The resulting high chamber pressure would make running the electron gun very difficult. Alloy formation must be prevented, even in small quantity, since the alloy is not epitaxial to CeO₂. If the alloy forms, the surface will not be lattice matched to any CeO₂ deposited on top of it. Likewise, deposition of oxygen deficient phases such as Ce₂O₃ or CeO must also be avoided to preserve the epitaxial surface. If the oxygen level is too high, the nickel substrate will oxidize, again covering the epitaxial nickel surface with a non-epitaxial contaminant.

Deposition of CeO_2 from a CeO_2 source on oxides is far simpler. The surface of an oxide substrate is not destroyed by increased oxygen partial pressure in the background gas composition, therefore, the lattice match between film and substrate determines the quality of the epitaxial film (provided that the film is deposited at a high enough temperature to yield sufficient surface mobility of the deposited species for epitaxial growth). Deposition on oxides from a metallic source yields an epitaxial film provided that there is sufficient oxygen present in the chamber to oxidize the cerium metal before it coats the substrate surface. If highly reduced, non-epitaxial species, such as Ce_2O_3 , CeO , or cerium metal are deposited, they will destroy the epitaxy of the growing film.

CHAPTER 5: CONCLUSIONS

Cubic cerium oxide (CeO_2) may be deposited epitaxially on nickel substrates provided that the oxygen level in the chamber during deposition is maintained at the proper level. Electron beam evaporation from a CeO_2 source or reactive evaporation from a cerium metal source may be employed. Sufficient oxygen must be present in the background gas composition to ensure that the metallic cerium oxidizes prior to hitting the substrate when evaporating from a metallic source. The oxygen level must also be maintained at a low enough level such that the nickel substrate does not oxidize prior to deposition. The species arriving at the substrate surface is oxidized, not cerium metal when depositing epitaxial CeO_2 by reactive evaporation. Measures must be taken to ensure that both the condition of the substrate surface and the composition of the arriving material flux are controlled during reactive evaporation of cerium to form epitaxial CeO_2 buffer layers on nickel.

Epitaxial evaporation from an oxide source on nickel is possible provided that care is taken to avoid oxidizing the surface of the nickel substrate. Oxygen gas evolved from the deposition source itself as the source oxide is reduced contributes significant quantities of oxygen to the compositional makeup of the background gas during deposition. The formation of nickel oxide may be avoided and epitaxial growth of CeO_2 directly on nickel occurs if a sufficient amount of forming gas is used to compensate for this increase in the partial pressure of oxygen as a result of evolution from the source. Cerium metal may also be used to getter the excess oxygen evolved by the deposition source. The most important

factor effecting epitaxy is the condition of the substrate, not the composition of the arriving deposition flux during evaporation of CeO_2 onto a nickel substrate to form an epitaxial film.

Controlling the oxygen level in the chamber during reactive evaporation of cerium metal such that NiO formation is not possible and such that CeO_2 is stable is not an easy task. The gettering power of the cerium metal must be compensated for, requiring significant amounts of oxygen. A mix of forming gas and oxygen must be used to avoid formation of nickel oxide on the surface. The proper mix must be maintained or film epitaxy will be lost. This mix of gas also requires that the background pressure in the chamber be fairly high, making it difficult to maintain a stable beam from an electron gun. Therefore, evaporation from an oxide source is a more desirable processing route. Forming gas may be used to prevent the formation of nickel oxide, and no oxygen is required to form the cubic CeO_2 phase, eliminating the need for mixed gas. It should be possible to form an initial epitaxial oxide layer on the substrate if the deposition rate is low at the beginning of deposition, then once the surface is protected, the deposition rate may be increased to speed processing. The preferred method for deposition of CeO_2 buffer layers on nickel substrates for superconductor applications is evaporation from an oxide source, as opposed to reactive evaporation of cerium metal as a result of the larger process window involved during oxide deposition.

APPENDIX A: UV/VIS THICKNESS MACRO

The following is the macro code used to calculate film thicknesses from UV/Vis transmission spectra in Microsoft Excel version 7.0. The code was written using Microsoft Visual Basic for Applications.

The macro plots the original data and attempts to identify the extremes in the spectrum. It then allows the user to modify the extremes the computer has identified (since the peak finding algorithm is not perfect, manual intervention is sometimes necessary). Once the extremes have been identified, the values are exported to an external curve fitting program (Curve Expert v1.3) where the theoretical formula for the transmission envelopes is used to produce fits of the identified extremes. These fits and the identified extremes are then used to calculate a film refractive index and film thickness. The transmission spectrum is then formatted and printed.

```
'*****'
```

```
'Declare all variables.'
```

```
Option Base 1  
Option Explicit
```

```
Dim i As Integer, maxrows As Integer, maxfirst As Integer, lambmin() As Integer, _  
lambmax() As Integer, mins As Integer, totalrows As Integer, maxes As Integer, _  
maxlast As Integer, j As Integer, k As Integer, lambminref() As Integer, _  
lambmaxref() As Integer, minsref As Integer, maxesref As Integer, _  
skip As Integer, firstlamb As Integer, lastlamb As Integer, minrows As Integer, _  
fit As Integer, q As Integer
```

```
Dim delta() As Single, transmin() As Single, transmax() As Single, _  
mintrans As Single, maxtrans As Single, lamb() As Single, trans() As Single, _  
minco() As Double, maxco() As Double, coeffs(4) As Single, _  
extransmin() As Single, minscale As Single, extransmax() As Single, _  
nsub As Single, nfilm() As Single, x() As Double, thick As Single, _  
extlamb() As Single, tsub As Single
```

```
Dim dataname As String, origname As String, originalfile, reference, minlamb, _  
maxlamb, resmooth, oldvalues As Boolean, newHour, newMinute, newSecond
```

```
'*****'
```

```
'This is the main program which calls subroutines.'
```

```
Static Sub UVVISabs()  
i = MsgBox("Make sure Curve Expert is running!", vbOK, "Run Curve Expert")  
Set originalfile = Application.ActiveWorkbook  
origname = originalfile.Name  
ActiveWorkbook.SaveAs "e:\todd\abs\TEMP.TXT", FileFormat:=xlText  
dataname = "temp.txt"  
general  
preplot
```

```

maxmin
verify
q = 0
Windows("UVVIS thickness and plot.xls").Activate
If DialogSheets("Verify").Show Then
    export
    curvxprt
    applyfit
    calcs
    plot
End If
End Sub

```

```

'*****

```

```

'Dimension arrays.  Format the data for subsequent processing.

```

```

Static Sub general()

```

```

ReDim lambmin(20)
ReDim transmin(20)
ReDim lambmax(20)
ReDim transmax(20)
ReDim extlamb(40)
ReDim lambminref(20)
ReDim lambmaxref(20)

```

```

maxrows = ActiveSheet.UsedRange.Rows.count
Range(Cells(1, 1), Cells(4, 1)).Select
Selection.Cut
Range(Cells(6, 15), Cells(9, 15)).Select
ActiveSheet.Paste
Cells(10, 15).Value = origname
Rows("1:4").Select
Selection.Delete shift:=xlUp
maxrows = maxrows - 4

```

```

minrows = 1
totalrows = maxrows
nsub = 1
firstlamb = Cells(1, 1).Value
lastlamb = Cells(maxrows, 1).Value
minlamb = firstlamb
maxlamb = lastlamb
maxtrans = Application.max(ActiveSheet.Columns(2))
mintrans = Application.min(ActiveSheet.Columns(2))

```

```
End Sub
```

```
'*****
```

```
'Plot data so that the user can see it and decide what limits to use during
'processing.
```

```
Sub preplot()
Dim total As Single, temp As String, goodfit, n, reference As String, _
temp1 As Single, temp2 As Single, temp3 As Single
```

```

minlamb = firstlamb
maxlamb = lastlamb
    ActiveSheet.ChartObjects.Add(100, 5, 350, 250).Select
    Application.CutCopyMode = False
    reference = "A1:A" & totalrows & ",B1:B" & totalrows
    ActiveChart.ChartWizard Source:=Range(reference), Gallery:= _
        xlXYScatter, Format:=2, PlotBy:=xlColumns, CategoryLabels:=1, _
        SeriesLabels:=0, HasLegend:=1
    ActiveSheet.ChartObjects(1).Activate
    ActiveChart.Axes(xlCategory).Select
    With ActiveChart.Axes(xlCategory)
        .MinimumScale = Int(minlamb / 100) * 100
        .MaximumScale = Application.RoundUp(maxlamb / 100, 0) * 100
    End With
    ActiveChart.Axes(xlValue).Select

```

```

With ActiveChart.Axes(xlValue)
    .MinimumScale = 0
    .MaximumScale = 1
    .TickLabels.NumberFormat = "0.00"

End With
ActiveChart.Legend.Delete
ActiveChart.PlotArea.Select
Selection.Width = 340
ActiveChart.SeriesCollection(1).MarkerStyle = xlNone
With ActiveChart.SeriesCollection(1).Border
    .ColorIndex = 3
    .Weight = xlHairline
    .LineStyle = xlContinuous
End With
Worksheets(1).Activate
temp = InputBox("Enter minimum wavelength to use. Exclude values near " & _
    "the cutoff edge.", "Minimum Wavelength", 250)
If temp <> "" Then minlamb = CInt(temp)
If temp = "" Then End
temp = InputBox("Enter the maximum wavelength to use. It's a good idea " & _
    "to exclude at least the top two extrema.", "Maximum Wavelength", 1100)
If temp <> "" Then maxlamb = CInt(temp)
If temp = "" Then End
Worksheets(1).ChartObjects(1).Delete
End Sub

'*****

'Identify extrema. Load values into arrays. Two arrays are necessary to keep
'track of actual extrema and values used only for curve fitting.

Sub maxmin()

ReDim delta(5)
maxes = 0

```

```

mins = 0
For i = 4 To totalrows - 3
    delta(5) = Sgn(Cells(i + 3, 2).Value - Cells(i + 2, 2).Value)
    delta(4) = Sgn(Cells(i + 2, 2).Value - Cells(i + 1, 2).Value)
    delta(2) = Sgn(Cells(i - 1, 2).Value - Cells(i - 2, 2).Value)
    delta(1) = Sgn(Cells(i - 2, 2).Value - Cells(i - 3, 2).Value)
    If delta(5) = delta(4) And delta(2) = delta(1) And delta(4) <> delta(2) Then
        If delta(4) > delta(2) And Cells(i, 2).Value > 0.1 Then
            mins = mins + 1
            minsref = mins
            lambmin(mins) = Cells(i, 1).Value
            lambminref(mins) = Cells(i, 1).Value
            transmin(mins) = Cells(i, 2).Value
            i = i + 2
        End If
        If delta(4) < delta(2) And Cells(i, 2).Value > 0.1 Then
            maxes = maxes + 1
            maxesref = maxes
            lambmax(maxes) = Cells(i, 1).Value
            lambmaxref(maxes) = Cells(i, 1).Value
            transmax(maxes) = Cells(i, 2).Value
            i = i + 2
        End If
    End If
Next i
Range(Cells(1, 8), Cells(10, 11)).Clear
For i = 1 To 20
    If lambmax(i) <> 0 Then Cells(i, 8).Value = lambmax(i)
    If transmax(i) <> 0 Then Cells(i, 9).Value = transmax(i)
    If lambmin(i) <> 0 Then Cells(i, 10).Value = lambmin(i)
    If transmin(i) <> 0 Then Cells(i, 11).Value = transmin(i)
Next i
End Sub

```

'*****'

'Plot identified extrema and format the plot to facilitate modification of the
'extrema the computer identifies. Give a warning for probable locations where
'the same extreme has been identified twice.

```
Sub verify()  
Dim dummy As Integer  
ActiveSheet.ChartObjects.Add(250, 5, 300, 275).Select  
Application.CutCopyMode = False  
reference = "A1:A" & maxrows & ",B1:B" & maxrows  
ActiveChart.ChartWizard Source:=Range(reference),  
    Gallery:=xlXYScatter, Format:=2, PlotBy:=xlColumns, _  
    CategoryLabels:=1, SeriesLabels:=0, HasLegend:=1, _  
    Title:="UV/VIS Spectrum (" & Cells(3, 15).Value & ")", _  
    CategoryTitle:="Wavelength (nm)", ValueTitle:="Transmittance "
```



```
    ActiveSheet.ChartObjects(1).Activate  
    ActiveChart.Legend.Select  
    Selection.Delete  
    ActiveChart.PlotArea.Select  
    Selection.Width = 295  
    With Selection.Border  
        .ColorIndex = 1  
        .Weight = xlThin  
        .LineStyle = xlContinuous  
    End With  
    With Selection.Interior  
        .ColorIndex = 2  
        .PatternColorIndex = 1  
        .Pattern = xlSolid  
    End With  
    ActiveChart.SeriesCollection(1).MarkerStyle = xlNone  
    ActiveChart.SeriesCollection(1).Select  
    With Selection.Border  
        .ColorIndex = 1  
        .Weight = xlHairline
```

```
        .LineStyle = xlContinuous
End With
With ActiveChart.PageSetup
    .LeftHeader = ""
    .CenterHeader = ""
    .RightHeader = ""
    .LeftFooter = ""
    .CenterFooter = ""
    .RightFooter = ""
End With
```

```
Windows(dataname).Activate
Worksheets(1).Activate
ActiveChart.SeriesCollection.Add Source:=Range(Cells(1, 8), Cells(20, 9)), _
    Rowcol:=xlColumns, SeriesLabels:=False, CategoryLabels:=True, _
    Replace:=False
ActiveChart.SeriesCollection.Add Source:=Range(Cells(1, 10), Cells(20, 11)), _
    Rowcol:=xlColumns, SeriesLabels:=False, CategoryLabels:=True, _
    Replace:=False
```

```
ActiveSheet.ChartObjects(1).Activate
ActiveChart.Axes(xlCategory).Select
With ActiveChart.Axes(xlCategory)
    .MinimumScale = Int(firstlamb / 100) * 100
    .MaximumScale = Application.RoundUp(lastlamb / 100, 0) * 100
End With
```

```
ActiveChart.Axes(xlValue).Select
With ActiveChart.Axes(xlValue)
    .MinimumScale = Int(mintrans * 10) / 10
    .MaximumScale = 1
    .TickLabels.NumberFormat = "0.00"
```

```
End With
```

```
ActiveChart.SeriesCollection(1).MarkerStyle = xlNone
ActiveChart.SeriesCollection(1).Border.ColorIndex = 1
```

```
ActiveChart.SeriesCollection(2).Select
Selection.Border.LineStyle = xlNone
With Selection
    .MarkerBackgroundColorIndex = xlNone
    .MarkerForegroundColorIndex = 5
    .MarkerStyle = xlPlus
End With
```

```
ActiveChart.SeriesCollection(3).Select
Selection.Border.LineStyle = xlNone
With Selection
    .MarkerBackgroundColorIndex = xlNone
    .MarkerForegroundColorIndex = 3
    .MarkerStyle = xlX
End With
```

```
Worksheets(1).Activate
```

```
For i = 1 To mins - 1
    dummy = Application.RoundUp((lambmin(i) * 0.02), 0)
    If lambmin(i + 1) - lambmin(i) <= dummy Then
        dummy = MsgBox("There are two identified minima at " & lambmin(i) & _
            " and " & lambmin(i + 1) & " nm. Make sure there's only one " & _
            "point per extreme.", vbOKOnly, "Repeated Point?")
```

```
Next i
```

```
For i = 1 To maxes - 1
    dummy = Application.RoundUp((lambmax(i) * 0.02), 0)
    If lambmax(i + 1) - lambmax(i) < dummy Then
        dummy = MsgBox("There are two identified maxima at " & lambmax(i) & _
            " and " & lambmax(i + 1) & " nm. Make sure there's only one " & _
            "point per extreme.", vbOKOnly, "Repeated Point?")
```

```
Next i
```

End Sub

```
'*****
```

```
' Initialize the values in the dialog box which will allow changes to identified  
'extrema to be made.
```

```
Sub init()
```

```
Dim i As Integer, j As Integer
```

```
Windows("UVVIS thickness and plot.xls").Activate
```

```
DialogSheets("verify").DialogFrame.Left = 0
```

```
DialogSheets("verify").DialogFrame.Top = 0
```

```
For i = 4 To 43
```

```
    DialogSheets("verify").EditBoxes("edit box " & i).Text = Empty
```

```
Next i
```

```
For i = 1 To 10
```

```
    DialogSheets("verify").EditBoxes("edit box " & i + 3).Text = _  
        lambmax(i + (10 * q))
```

```
    DialogSheets("verify").EditBoxes("edit box " & i + 13).Text = _  
        Application.Round(transmax(i + (10 * q)), 4)
```

```
    DialogSheets("verify").EditBoxes("edit box " & (i + 23)).Text = _  
        lambmin(i + (10 * q))
```

```
    DialogSheets("verify").EditBoxes("edit box " & (i + 33)).Text = _  
        Application.Round(transmin(i + (10 * q)), 4)
```

```
Next i
```

```
If q = 0 Then
```

```
    DialogSheets("Verify").Buttons("Button 57").Enabled = True
```

```
    DialogSheets("Verify").Buttons("Button 58").Enabled = False
```

```
ElseIf q = 1 Then
```

```
    DialogSheets("Verify").Buttons("Button 57").Enabled = False
```

```
    DialogSheets("Verify").Buttons("Button 58").Enabled = True
```

```
End If
```

```
Windows(dataname).Activate
```

End Sub

'*****

'Allow changes to the extrema identified. Update the appropriate arrays,
'spreadsheet cells, and dialog box entries.

Sub update()

Dim temp, dummy

Windows("UVVIS thickness and plot.xls").Activate

Dim i As Integer

For i = 1 To 10

If DialogSheets("Verify").EditBoxes("edit box " & i + 3).Text = "" Or _
DialogSheets("Verify").EditBoxes("edit box " & i + 13).Text = "" Or _
DialogSheets("Verify").EditBoxes("edit box " & i + 23).Text = "" Or _
DialogSheets("Verify").EditBoxes("edit box " & i + 33).Text = "" Then

temp = MsgBox("You can't leave any blank selections in the wavelength" & _
"/transmission box. Please fill in blanks with zeros and try again.", _
vbOK, "Try Again")

Exit Sub

End If

Next i

For i = 1 To 10

'the following if block kills a value that was non-zero on the dialogbox but
'was changed to zero by the user. The value is deleted from both lambmax and
'lambmaxref. If the value haschanged from zero to non-zero value, the user is
'questioned whether the pointis only for fitting, then lambmax and lambmaxref
'are updated appropriately.

'First, if a dialogbox value is zero and it wasn't to begin with

'(so lambmax(i)<>0) then remove the value from both lambmax and lambmaxref.

If DialogSheets("Verify").EditBoxes("edit box " & i + 3).Text <> _
lambmax(i + (10 * q)) Then

If DialogSheets("Verify").EditBoxes("edit box " & i + 3).Text = "0" Then

```

For k = 1 To 10
    If lambmax(i + (10 * q)) = lambmaxref(k + (10 * q)) Then
        lambmaxref(k + (10 * q)) = 0
        Exit For
    End If
Next k
lambmax(i + (10 * q)) = 0
'If the value in the dialogbox has changed either from one non-zero value from
'another or from zero to a non-zero value, then check the status of added points
'and update lambda arrays with additions or changes.
    ElseIf DialogSheets("Verify").EditBoxes("edit box " & i + 3).Text <
    > "0" Then
        temp = vbYes
'Check to see that any added points are really peaks, not just supplemental
'fitting points.
    If lambmax(i + (10 * q)) = 0 Then
        dummy = DialogSheets("Verify").EditBoxes
            ("edit box " & i + 3).Text
        Windows(dataname).Activate
        temp = MsgBox("You added a point at " & dummy & "nm to use" &
            "while fitting the maxima. Is it an actual peak value? " &
            "(not just a supplemental point)", vbYesNo + vbDefaultButton1,
            "Peak or Supplemental?")
    End If
'if an added point really is a peak value or if a value has changed,
'update lambmaxref. Keep in mind...to get into this if block, the dialogbox
'value has changed. All values in lambmaxref should exist in lambmax at this point.
    Windows("UVVIS thickness and plot.xls").Activate
    If temp <> vbNo Then
        For k = 1 To 10
            'the following if simply finds the right value to change in
            'lambmaxref since the counter in that array is not synchronous
            'with i. We already KNOW that the arrays need updating at this
            'point...just finding the right value to change. Once we've
            'found and updated the right point, pop out of the loop.
            If lambmax(i + (10 * q)) = lambmaxref(k + (10 * q)) Then

```

```

        lambmaxref(k + (10 * q)) = DialogSheets("Verify"). _
            EditBoxes("edit box " & i + 3).Text
    Exit For
End If
Next k
End If
'Regardless of whether or not a non-zero value in the dialogbox corresponds to a
'peak in the spectrum, it MUST go into lambmax so that it will be used for fitting.
    lambmax(i + (10 * q)) = DialogSheets("Verify").EditBoxes _
        ("edit box " & i + 3).Text
End If
End If
'all transmax values in the dialogbox may be updated in transmax. They all get
'used for fits anyway, and later the necessary transmission values will be
'calculated from the fits, not taken from the real data, so there's no need for a
'transmaxref array.
    If DialogSheets("Verify").EditBoxes("edit box " & i + 13).Text <> _
        transmax(i + (10 * q)) Then transmax(i + (10 * q)) = DialogSheets _
            ("Verify").EditBoxes("edit box " & i + 13).Text
'Repeat the above scheme for the minima in the dialogbox.
    If DialogSheets("Verify").EditBoxes("edit box " & i + 23).Text <> _
        lambmin(i + (10 * q)) Then
        If DialogSheets("Verify").EditBoxes("edit box " & i + 23).Text = "0" Then
            For k = 1 To 10
                If lambmin(i + (10 * q)) = lambminref(k + (10 * q)) Then
                    lambminref(k + (10 * q)) = DialogSheets("Verify").EditBoxes _
                        ("edit box " & i + 23).Text
                Exit For
            End If
        Next k
        lambmin(i + (10 * q)) = DialogSheets("Verify").EditBoxes _
            ("edit box " & i + 23).Text
    ElseIf DialogSheets("Verify").EditBoxes("edit box " & i + 23).Text _
        <> "0" Then
        temp = vbYes
        If lambmin(i + (10 * q)) = 0 Then

```

```

        dummy = DialogSheets("Verify").EditBoxes _
            ("edit box " & i + 23).Text
        Windows(dataname).Activate
        temp = MsgBox("You added a point at " & dummy & "nm to use " & _
            "while fitting the minima. Is it an actual valley value? " & _
            "(not just a supplemental point)", vbYesNo + vbDefaultButton1, _
            "Valley or Supplemental?")
    End If
    Windows("UVVIS thickness and plot.xls").Activate
    If temp <> vbNo Then
        For k = 1 To 10
            If lambmin(i + (10 * q)) = lambminref(k + (10 * q)) Then
                lambminref(k + (10 * q)) = DialogSheets("Verify"). _
                    EditBoxes("edit box " & i + 23).Text
            Exit For
        End If
    Next k
    End If
    lambmin(i + (10 * q)) = DialogSheets("Verify").EditBoxes _
        ("edit box " & i + 23).Text
    End If
End If
If DialogSheets("Verify").EditBoxes("edit box " & i + 33).Text <> _
    transmin(i + (10 * q)) Then
    transmin(i + (10 * q)) = DialogSheets("Verify").EditBoxes _
        ("edit box " & i + 33).Text
Next i

Windows(dataname).Activate
'Load the proper cell values to update the plot. Assign them the empty
'value if appropriate.
For i = 1 To 20
If lambmax(i) <> 0 Then Cells(i, 8).Value = lambmax(i) Else _
    Cells(i, 8).Value = Empty
If lambmax(i) <> 0 Then Cells(i, 9).Value = transmax(i) Else _
    Cells(i, 9).Value = Empty

```

```

If lambmin(i) <> 0 Then Cells(i, 10).Value = lambmin(i) Else _
    Cells(i, 10).Value = Empty
If lambmin(i) <> 0 Then Cells(i, 11).Value = transmin(i) Else _
    Cells(i, 11).Value = Empty
Next i

```

```
End Sub
```

```
'*****
```

```
'Sort the extrema just identified, place them on individual sheets in the workbook.
'Export the extrema identified to text files which may be read by the curve
'fitting program. Also, write a recovery file in case the macro crashes during
'processing so that the extrema do not need to be identified again next time.

```

```

Sub export()
Dim cntr1 As Integer, cntr2 As Integer
cntr1 = 1
cntr2 = 1
Sheets.Add
Sheets.Add
Sheets.Add
Sheets(4).Move Before:=Sheets(1)
Sheets(4).Move Before:=Sheets(2)
Sheets(4).Move Before:=Sheets(3)
Worksheets(1).Activate
For i = 1 To 20
    If lambmaxref(i) <> 0 Then Cells(i, 6).Value = lambmaxref(i) Else _
        Cells(i, 6).Value = Empty
    If lambminref(i) <> 0 Then Cells(i, 7).Value = lambminref(i) Else _
        Cells(i, 7).Value = Empty
Next i

```

```

Columns("F").Select
Selection.Sort Key1:=Range("F1"), Order1:=xlAscending, Header:= _
    xlGuess, OrderCustom:=1, MatchCase:=False, Orientation:= _

```

xlTopToBottom

```
Columns("G").Select
Selection.Sort Key1:=Range("G1"), Order1:=xlAscending, Header:= _
xlGuess, OrderCustom:=1, MatchCase:=False, Orientation:= _
xlTopToBottom
```

```
Columns("H:I").Select
Selection.Sort Key1:=Range("H1"), Order1:=xlAscending, Header:= _
xlGuess, OrderCustom:=1, MatchCase:=False, Orientation:= _
xlTopToBottom
```

```
Columns("J:K").Select
Selection.Sort Key1:=Range("J1"), Order1:=xlAscending, Header:= _
xlGuess, OrderCustom:=1, MatchCase:=False, Orientation:= _
xlTopToBottom
```

```
cntr1 = 1
cntr2 = 1
For i = 1 To 20
If Cells(i, 9).Value <> 0 Then
    Worksheets(2).Cells(cntr1, 1).Value = Cells(i, 8).Value
    Worksheets(2).Cells(cntr1, 2).Value = Cells(i, 9).Value
    cntr1 = cntr1 + 1
End If
If Cells(i, 11).Value <> 0 Then
    Worksheets(3).Cells(cntr2, 1).Value = Cells(i, 10).Value
    Worksheets(3).Cells(cntr2, 2).Value = Cells(i, 11).Value
    cntr2 = cntr2 + 1
End If
Next i
```

```
Range(Cells(1, 6), Cells(20, 11)).Select
Selection.Copy
Sheets(4).Select
Range(Cells(1, 1), Cells(20, 6)).Select
```

```

ActiveSheet.Paste
Range("A1").Select
Sheets(1).Select
Worksheets(2).SaveAs filename:="e:\todd\abs\maxes.dat", FileFormat:=xlText
Worksheets(3).SaveAs filename:="e:\todd\abs\mins.dat", FileFormat:=xlText
Worksheets(4).SaveAs filename:="e:\todd\abs\crash.txt", FileFormat:=xlText
Worksheets(1).SaveAs filename:="e:\todd\abs\" & dataname, FileFormat:=xlText
End Sub

```

```

'*****

```

```

'Run the curve fitting program by sending key commands to carry out the appropriate
'fitting functions.

```

```

Sub curvxprt()

```

```

Dim dummy As Single, currentime As Single, waitime As Date, actap, delay As Integer

```

```

For i = 1 To 2

```

```

    actap = Shell("c:\curvxprt\cvxprt32.exe", 1)

```

```

    currentime = CSng(Time)

```

```

    waitime = CDate(currentime + (1 / 86400))

```

```

    Application.Wait (waitime)

```

```

    AppActivate "CurveExpert 1.3"

```

```

    currentime = CSng(Time)

```

```

    waitime = CDate(currentime + (1 / 86400))

```

```

    Application.Wait (waitime)

```

```

    SendKeys "%fo", True

```

```

    If i = 1 Then SendKeys "e:\todd\abs\maxes.dat", True

```

```

    If i = 2 Then SendKeys "e:\todd\abs\mins.dat", True

```

```

    SendKeys "~~", True

```

```

    SendKeys "%dmx0.001~%{F4}", True

```

```

    If i = 1 Then SendKeys "%au{TAB}{DOWN 8}~1.1{DOWN}0.04{DOWN}-1.7{DOWN}" & _
        "-0.1{DOWN}5.6{DOWN}-0.04{UP}{TAB 3}~" 'True

```

```

    If i = 2 Then SendKeys "%au{TAB}{DOWN 8}~1.0{DOWN}0.02{DOWN}-1.8{DOWN}" & _
        "-0.1{DOWN}4.3{DOWN}-0.04{UP}{TAB 3}~" 'True

```

```

currentime = CSng(Time)
waitime = CDate(currentime + (5 / 86400))
Application.Wait (waitime)
delay = CInt(MsgBox("Hit OK when CurveExpert is done", vbOKOnly, "Finished?"))
AppActivate "User-Defined Model"
    currentime = CSng(Time)
    waitime = CDate(currentime + (1 / 86400))
    Application.Wait (waitime)
SendKeys "^i", True
SendKeys "pc%{F4}", True
AppActivate "CurveExpert 1.3"
    currentime = CSng(Time)
    waitime = CDate(currentime + (1 / 86400))
    Application.Wait (waitime)
SendKeys "%fnn", True
AppActivate "Microsoft Excel"
If i = 1 Then Cells(25, 7).Select
If i = 2 Then Cells(25, 9).Select
ActiveSheet.Paste
Next i

End Sub

'*****
'Use the fit parameters to generate columns of plot-ready data. Place the curve
'fits onto the master plot of the transmission spectrum.

Sub applyfit()
Dim a As Double, b As Double, c As Double, d As Double, e As Double, f As Double
ReDim minco(6)
ReDim maxco(6)

For j = 1 To 2
    If j = 1 Then
        For i = 1 To 6

```

```

        maxco(i) = Cells(26 + i, 8).Value
    Next i
    a = maxco(1)
    b = maxco(2)
    c = maxco(3)
    d = maxco(4)
    e = maxco(5)
    f = maxco(6)
ElseIf j = 2 Then
    For i = 1 To 6
        minco(i) = Cells(26 + i, 10).Value
    Next i
    a = minco(1)
    b = minco(2)
    c = minco(3)
    d = minco(4)
    e = minco(5)
    f = minco(6)

End If

```

88

```

Range(Cells(1, 1), Cells(totalrows, 1)).Select
Selection.Copy
Cells(1, 12).Select
ActiveSheet.Paste
    For i = 1 To totalrows
        Cells(i, 12 + j).Value = (a * (e * Exp(f * Exp(1.24 /
            (Cells(i, 12).Value / 1000)))) / (b - (c * (e * Exp(f * Exp
            (1.24 / (Cells(i, 12).Value / 1000)))))) + (d * (e * Exp
            (f * Exp(1.24 / (Cells(i, 12).Value / 1000)))) ^ 2))
    Next i
Next j

ActiveSheet.ChartObjects(1).Activate

```

```

Application.CutCopyMode = False
ActiveChart.SeriesCollection.Add Source:="[TEMP.TXT]TEMP!$L$1:$N$901", _
    Rowcol:=xlColumns, SeriesLabels:=False, CategoryLabels:=True, _
    Replace:=False

ActiveSheet.ChartObjects(1).Activate
ActiveChart.SeriesCollection(4).Select

With Selection.Border
    .ColorIndex = 1
    .Weight = xlHairline
    .LineStyle = xlDot
End With
Selection.MarkerStyle = xlNone

ActiveChart.SeriesCollection(5).Select
With Selection.Border
    .ColorIndex = 1
    .Weight = xlHairline
    .LineStyle = xlDot
End With
Selection.MarkerStyle = xlNone

Worksheets(1).Activate
End Sub

'*****

'Calculate the film thickness. Allow user to monitor the calculations (with
'plots) and enter necessary values when appropriate. Format relevant data on
'the spreadsheet.

Sub calcs()
Dim capn As Single, cape As Single, tempm, choice As Integer, m As Single, _
fit() As Single, max As Integer, min As Integer, nomin As Integer, _
nomax As Integer, totalextrêmes As Integer, maxmin As Integer, maxmax As Integer, _

```

a As Double, b As Double, c As Double, d As Double, e As Double, f As Double, _
repeat As Boolean

```
nommin = 0
nommax = 0
For i = 1 To 20
    If lambminref(i) >= minlamb And nommin = 0 Then
        min = i
        nommin = 1
    End If
    If lambmaxref(i) >= maxlamb And nommax = 0 Then
        max = i
        nommax = 1
    End If
Next i
```

06

```
k = 1
For i = 1 To 20
    If lambminref(i) >= minlamb And lambminref(i) <= maxlamb Then
        Cells(2 + k, 16).Value = lambminref(i)
        maxmin = lambminref(i)
        k = k + 1
    End If
    If lambmaxref(i) >= minlamb And lambmaxref(i) <= maxlamb Then
        Cells(2 + k, 16).Value = lambmaxref(i)
        maxmax = lambmaxref(i)
        k = k + 1
    End If
Next i
```

```
Range(Cells(3, 16), Cells(43, 16)).Sort Key1:=Columns(16)
k = 1
For i = 1 To 40
    If Cells(i + 2, 16).Value <> 0 And Not (IsEmpty(Cells(i + 2, 16))) Then
        extlamb(k) = Cells(i + 2, 16).Value
```

```

        k = k + 1
    End If
Next i
totalextrêmes = k - 1

ReDim extransmin(totalextrêmes)
ReDim extransmax(totalextrêmes)
ReDim nfilm(totalextrêmes)
ReDim x(totalextrêmes)
ReDim fit(totalextrêmes)

For j = 1 To 2
    If j = 1 Then
        a = maxco(1)
        b = maxco(2)
        c = maxco(3)
        d = maxco(4)
        e = maxco(5)
        f = maxco(6)
    ElseIf j = 2 Then
        a = minco(1)
        b = minco(2)
        c = minco(3)
        d = minco(4)
        e = minco(5)
        f = minco(6)
    End If
For i = 1 To totalextrêmes
    fit(i) = (a * (e * Exp(f * Exp(1.24 / (extlamb(i) / 1000)))) /
        (b - (c * (e * Exp(f * Exp(1.24 / (extlamb(i) / 1000)))) +
        (d * (e * Exp(f * Exp(1.24 / (extlamb(i) / 1000)))) ^ 2))
Next i

Cells(1, 23).Value = "transmax"
Cells(1, 22).Value = "transmin"
For i = 1 To totalextrêmes

```

```

    If j = 1 Then
        extransmax(i) = fit(i)
        Cells(i + 2, 23).Value = extransmax(i)
    End If
    If j = 2 Then
        extransmin(i) = fit(i)
        Cells(i + 2, 22).Value = extransmin(i)
    End If
Next i
Next j

Cells(1, 17).Value = "nfilm(1)"
For i = 1 To totalextremes
    capn = (2 * nsub * ((extransmax(i) - extransmin(i)) / _
        (extransmax(i) * extransmin(i)))) + (((nsub ^ 2) + 1) / 2)
    nfilm(i) = (capn + ((capn ^ 2) - (nsub ^ 2)) ^ 0.5) ^ 0.5
    Cells(i + 2, 17).Value = nfilm(i)
Next i

Cells(1, 20).Value = "n/lamb"
Cells(1, 21).Value = "l/2"
For i = 1 To totalextremes
    Cells(i + 2, 20).Value = nfilm(i) / extlamb(i)
    Cells(i + 2, 21).Value = (totalextremes - i) / 2
Next i

    Cells(1, 24).Value = "abs co"
    Cells(1, 25).Value = "energy"
    Cells(1, 26).Value = "ln(abs co)"
    Cells(1, 18).Value = "nfilm2"
    Cells(1, 19).Value = "fit nfilm"
    Cells(1, 16).Value = "wavelength"

Range(Cells(3, 16), Cells(23, 19)).Select
ActiveSheet.ChartObjects.Add(560, 10, 350, 250).Select
ActiveChart.ChartWizard Source:=Range("P3:S10"), Gallery:= _

```

```
xlXYScatter, Format:=2, PlotBy:=xlColumns, CategoryLabels:=1, _  
SeriesLabels:=0, HasLegend:=1
```

```
ActiveSheet.ChartObjects(2).Activate  
Windows(dataname).Activate
```

```
repeat = True  
Do While repeat = True  
    Range(Cells(2, 18), Cells(23, 19)).Clear  
    Range(Cells(2, 24), Cells(23, 26)).Clear  
    m = (Application.Intercept(Range(Cells(3, 21), Cells(43, 21)), _  
        Range(Cells(3, 20), Cells(43, 20))))  
    If maxmax > maxmin Then  
        tempm = Application.Round(m, 0)  
        choice = MsgBox("Calculating intercept. The intercept should " & _  
            "be an exact integer value. The actual value calculated is " & _  
            m & ". Using " & tempm & ". Is this correct?", vbYesNo + _  
            vbDefaultButton1, "Verify Intercept")  
    ElseIf maxmax < maxmin Then  
        tempm = Int(m) + 0.5  
        choice = MsgBox("Calculating intercept. The intercept should " & _  
            "be an exact half integer value. The actual value calculated " & _  
            "is " & m & ". Using " & tempm & ". Is this correct?", _  
            vbYesNo + vbDefaultButton1, "Verify Intercept")  
    End If  
    If choice = vbNo Then  
        tempm = InputBox("Enter correct intercept value (calculated value" & _  
            " = " & m & ".", "Enter intercept")  
    m = tempm  
    Cells(2, 20).Value = 0  
    Cells(2, 21).Value = m  
    thick = Application.Slope(Range(Cells(2, 21), Cells(42, 21)), _  
        Range(Cells(2, 20), Cells(42, 20))) / 2 * 10  
    Cells(2, 17).Value = thick
```

```

For i = 1 To totalextremes
    nfilm(i) = extlamb(i) * (-m + (totalextremes - i) / 2) / (2 * (thick / 10))
    Cells(i + 2, 18).Value = nfilm(i)
    Cells(i + 2, 3).Value = 1 / (extlamb(i) ^ 2)
Next i

a = Application.Slope(Range(Cells(3, 18), Cells(3 + totalextremes, 18)), _
    Range(Cells(3, 3), Cells(3 + totalextremes, 3)))
b = Application.Intercept(Range(Cells(3, 18), Cells(3 + totalextremes, 18)), _
    Range(Cells(3, 3), Cells(3 + totalextremes, 3)))
Range(Cells(3, 3), Cells(43, 3)).Clear

For i = 1 To totalextremes
    nsub = (2 * (0.0000534952 * extlamb(i) + 0.891155285)) / _
        ((0.0000534952 * extlamb(i) + 0.891155285) ^ 2 + 1)
    nfilm(i) = (a * (1 / extlamb(i) ^ 2)) + b
    cape = ((8 * (nfilm(i) ^ 2) * nsub) / extransmax(i)) + _
        ((nfilm(i) ^ 2 - 1) * ((nfilm(i) ^ 2) - (nsub ^ 2)))
    x(i) = (cape - (cape ^ 2 - ((nfilm(i) ^ 2 - 1) ^ 3) * (nfilm(i) ^ 2 - _
        nsub ^ 4)) ^ 0.5) / _
        (((nfilm(i) - 1) ^ 3) * (nfilm(i) - nsub ^ 2))
    Cells(i + 2, 24).Value = (-Log(x(i)) / (thick / 10)) / 0.0000001
    Cells(i + 2, 25).Value = (6.626E-34 * (300000000 / (extlamb(i) * _
        0.000000001))) / 1.602E-19
    Cells(i + 2, 26).Value = Log(Cells(i + 2, 24).Value)
    Cells(i + 2, 19).Value = nfilm(i)
Next i

choice = MsgBox("The refractive index shown in the graph should be " & _
    "parabolic and decreasing. If it's not, you probably have the " & _
    "wrong intercept value. Keep this intercept (" & m & ")?", vbYesNo _
    + vbDefaultButton1, "Verify Index Behavior")
If choice = vbYes Then repeat = False
Loop

```

```

Cells(2, 18).Value = "<-thickness"
Range(Cells(25, 7), Cells(32, 10)).Select
Selection.Copy
Range(Cells(1, 27), Cells(8, 30)).Select
ActiveSheet.Paste
End Sub

```

```

'*****

```

```

'Make final modifications to the transmission spectrum (including addition of the
'calculated thickness) and give the user the option of plotting it.

```

```

Sub plot()

```

```

Dim plot, thick

```

```

thick = CStr(Application.Round(Cells(2, 17).Value, 0))

```

```

For i = 9 To 11 Step 2

```

```

    For j = 1 To 20

```

```

        If Cells(j, i).Value = 0 And Cells(j, i - 1).Value <> Empty Then

```

```

            Cells(j, i).Value = 0.5

```

```

        ElseIf Cells(j, i - 1).Value = Empty Then

```

```

            Cells(j, i).Value = Empty

```

```

        End If

```

```

    Next j

```

```

Next i

```

```

ActiveSheet.ChartObjects(1).Select

```

```

    Selection.Left = 50

```

```

    Selection.Top = 10

```

```

    Selection.Width = 450

```

```

    Selection.Height = 250

```

```

ActiveSheet.ChartObjects(1).Activate

```

```

ActiveChart.PlotArea.Select
Selection.Width = 400

ActiveChart.ChartTitle.Font.Size = 14
ActiveChart.Axes(xlValue).AxisTitle.Font.Size = 12
ActiveChart.Axes(xlValue).TickLabels.Font.Size = 12
ActiveChart.Axes(xlCategory).AxisTitle.Font.Size = 12
ActiveChart.Axes(xlCategory).TickLabels.Font.Size = 12

ActiveChart.Axes(xlValue).Select
With ActiveChart.Axes(xlValue)
    .MinimumScale = 0.4
    .MaximumScale = 1
End With

ActiveChart.Axes(xlCategory).Select
With ActiveChart.Axes(xlCategory)
    .MinimumScale = 200
    .MaximumScale = 1100
End With

ActiveChart.TextBoxes.Add(290, 180, 200, 20).Select
Selection.Interior.ColorIndex = xlNone
Selection.Characters.Text = "Thickness= " & thick & " Angstroms"
Selection.Font.Size = 14
ActiveChart.PlotArea.Select

plot = MsgBox("Do you want to print this plot?", vbYesNo + vbDefaultButton1, _
    "Print?")
If plot = vbYes Then ActiveChart.PrintOut Copies:=1
End Sub

'*****

'This macro runs when the "<-BACK" button on the dialogsheet is pressed. It loads
'the previous 10 identified extrema into the dialogbox.

```

```
Sub backbutton()  
update  
q = 0  
init  
End Sub
```

```
'*****
```

```
'This macro runs when the "MORE->" button on the dialogsheet is pressed. It loads  
'the next 10 identified extrema into the dialogbox.
```

```
Sub morebutton()  
update  
q = 1  
init  
End Sub
```

```
'*****
```

```
'This macro runs when the "PV" (previous values) button on the dialogsheet  
'is pressed. This function is useful when a small modification to the previous  
'extrema is required or when something goes wrong and the program crashes in the  
'middle of curve fitting. The ability to reload previous values saves the time  
'and tedium of entering the values again.
```

```
Sub pvbutton()
```

```
Dim supps As Integer, real As Integer, j As Integer  
ReDim lambmax(20)  
ReDim lambmin(20)  
ReDim lambmaxref(20)  
ReDim lambminref(20)  
ReDim transmax(20)  
ReDim transmin(20)
```

```

Workbooks.OpenText filename:="E:\TODD\ABS\crash.txt", Origin:=
    xlWindows, StartRow:=1, DataType:=xlDelimited, TextQualifier _
    :=xlDoubleQuote, ConsecutiveDelimiter:=False, Tab:=True, _
    Semicolon:=False, Comma:=False, Space:=False, Other:=False, _
    FieldInfo:=Array(1, 1)

For i = 1 To 20
    lambmaxref(i) = CSng(Workbooks("crash.txt").Worksheets(1).Cells(i, 1).Value)
    lambminref(i) = CSng(Workbooks("crash.txt").Worksheets(1).Cells(i, 2).Value)
    lambmax(i) = CInt(Workbooks("crash.txt").Worksheets(1).Cells(i, 3).Value)
    transmax(i) = CSng(Workbooks("crash.txt").Worksheets(1).Cells(i, 4).Value)
    lambmin(i) = CInt(Workbooks("crash.txt").Worksheets(1).Cells(i, 5).Value)
    transmin(i) = CSng(Workbooks("crash.txt").Worksheets(1).Cells(i, 6).Value)
Next i

Windows("crash.txt").Close
Windows(dataname).Activate
init
update

End Sub

'*****

'This macro runs when the "DEF" (default) button on the dialogsheet is pressed.
'A set of generic extreme values are loaded into the spreadsheet. This is
'usefull when the peak finding algorithm fails miserably and hand entry of the
'extrema is required.

Sub defaultbutton()

Dim supps As Integer, real As Integer, j As Integer, maxin As Single, _
minin As Single, maxnm As Integer, minnm As Integer, temp As Single _

Workbooks.OpenText filename:="E:\TODD\ABS\default.txt", Origin:= _
    xlWindows, StartRow:=1, DataType:=xlDelimited, TextQualifier _

```

```
:=xlDoubleQuote, ConsecutiveDelimiter:=False, Tab:=True, _  
Semicolon:=False, Comma:=False, Space:=False, Other:=False, _  
FieldInfo:=Array(1, 1)
```

```
maxnm = 0  
maxin = 0  
minnm = 0  
minin = 0
```

```
Do
```

```
ReDim lambmax(20)  
ReDim lambmin(20)  
ReDim lambmaxref(20)  
ReDim lambminref(20)  
ReDim transmax(20)  
ReDim transmin(20)
```

```
For i = 1 To 9
```

```
    If CInt(Workbooks("default.txt").Worksheets(1).Cells(i, 1).Value)  
        + maxnm >= 200 Then lambmax(i + 5) = CInt(Workbooks("default.txt") _  
            .Worksheets(1).Cells(i, 1).Value) + maxnm  
    transmax(i + 5) = CSng(Workbooks("default.txt").Worksheets(1) _  
        .Cells(i, 2).Value) + maxin  
    If CInt(Workbooks("default.txt").Worksheets(1).Cells(i, 3).Value)  
        + minnm >= 200 Then lambmin(i + 5) = CInt(Workbooks("default.txt") _  
            .Worksheets(1).Cells(i, 3).Value) + minnm  
    transmin(i + 5) = CSng(Workbooks("default.txt").Worksheets(1) _  
        .Cells(i, 4).Value) + minin
```

```
Next i
```

```
Windows(dataname).Activate
```

```
init
```

```
update
```

```
j = 0
```

```
temp = CSng(InputBox("How does the fit to the maxima look?  If you " & _  
    "need to shift the maxima fit right or left, type the wavelength " & _  
    "shift below.  Otherwise, leave it at zero.", "Maxima wavelength shift", 0))
```

```

    If temp <> 0 Then
    maxnm = maxnm + temp
    j = 1
    End If
temp = CSng(InputBox("How does the fit to the maxima look?  If you need " & _
    "to shift the maxima fit up or down, type the intensity shift below.  " & _
    "Otherwise, leave it at zero.", "Maxima intensity shift", 0))
    If temp <> 0 Then
    maxin = maxin + temp
    j = 1
    End If
temp = CSng(InputBox("How does the fit to the minima look?  If you need " & _
    "to shift the minima fit right or left, type the wavelength shift " & _
    "below.  Otherwise, leave it at zero.", "Minima wavelength shift", 0))
    If temp <> 0 Then
    minnm = minnm + temp
    j = 1
    End If
temp = CSng(InputBox("How does the fit to the minima look?  If you need " & _
    "to shift the minima fit up or down, type the intensity shift below.  " & _
    "Otherwise, leave it at zero.", "Minima intensity shift", 0))
    If temp <> 0 Then
    minin = minin + temp
    j = 1
    End If

If j = 0 Then Exit Do
Loop

Windows("default.txt").Close
j = CInt(MsgBox("Realize that you have NO actual peak or valley values " & _
    "identified now!!", vbOK, "WARNING!!"))

End Sub

```

```

!*****

```

APPENDIX B: OXYGEN EVOLUTION FROM A CeO₂ SOURCE

In order to calculate the amount of oxygen introduced into the chamber atmosphere per unit time as a result of evolution from the source, it is necessary to first determine the total amount of material evaporated from the source per unit time.

The flux of material passing through a given area multiplied by the deposition rate of material through that area per unit time will give the volume of material deposited on that area per unit time.

$$dV = (R)(dA) \quad \text{where } dV = \text{volume deposited per unit time (cm}^3/\text{min)}$$

$$R = \text{deposition rate (length/time)}$$

$$dA = \text{element of area (cm}^2\text{)}$$

In order to carry out this calculation, envision a hemispherical surface over the electron gun source. Integrating the area of this hemisphere multiplied by the appropriate deposition rate at each point on the hemisphere will yield the total volume of material evaporated from the source.

The deposition profile from the electron gun is assumed to vary with angle from the source with a cosine distribution, such that the maximum deposition rate is directly above the source and drops to zero at right angles to the source. ($R = R_o \cos(\theta)$)

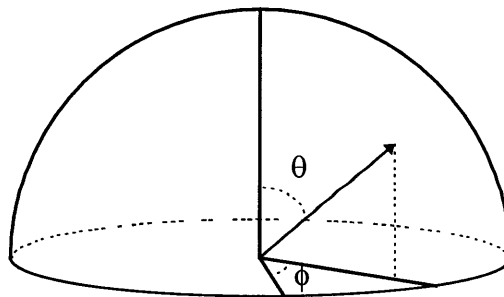
$$A = \iint r^2 d\theta \sin\theta \, d\phi$$

$$V = \iint (R_o \cos\theta)(r^2 d\theta \sin\theta \, d\phi)$$

$$V = R_o r^2 \iint \cos\theta \sin\theta \, d\theta \, d\phi$$

$$V = R_o r^2 \phi \Big|_0^{2\pi} \int \cos\theta \sin\theta \, d\theta$$

$$V = 2\pi R_o r^2 \int \cos\theta \sin\theta \, d\theta$$



From the CRC Handbook of Chemistry and Physics,⁴⁸

$$\int \cos(ax) \sin(ax) dx = \frac{1}{2a} \sin^2(ax)$$

$$\text{so } V = 2\pi R_o r^2 \left(\frac{1}{2} \sin\theta \Big|_0^{\pi/2} \right) = 2\pi R_o r^2 \left(\frac{1}{2} \right) = R_o \pi r^2$$

When the source is running, $R_{(\theta=18)} = 0.91 \text{ \AA/s}$ (see figure 3.10). The distance from the source to the rate monitor is 39cm.

First, the deposition rate must be given in cm/min.

$$\left(\frac{0.91 \text{ \AA}}{\text{sec}}\right) \left(\frac{1 \text{ cm}}{1 \times 10^8 \text{ \AA}}\right) \left(\frac{60 \text{ sec}}{\text{min}}\right) = 5.46 \times 10^{-7} \text{ cm/min } @ \theta = 18^\circ$$

$$\left(\frac{5.46 \times 10^{-7} \text{ cm}}{\text{min}}\right) \left(\frac{1}{\cos(18^\circ)}\right) = 5.74 \times 10^{-7} \text{ cm/min} = R_o$$

Total volume of CeO_2 per minute from the source = $\pi R_o r^2$.

$$\pi (5.74 \times 10^{-7}) (39 \text{ cm})^2 = 2.74 \times 10^{-3} \text{ cm}^3 / \text{min}$$

Total moles CeO_2 :

$$\left(\frac{2.74 \times 10^{-3} \text{ cm}^3}{\text{min}}\right) \left(\frac{7.132 \text{ g CeO}_2}{\text{cm}^3 \text{ CeO}_2}\right) \left(\frac{1 \text{ mole CeO}_2}{172.12 \text{ g CeO}_2}\right) = 1.14 \times 10^{-4} \text{ moles CeO}_2 / \text{min}$$

Total oxygen evolved depends on the amount of reduction occurring at the source. Assume that stoichiometry of deposited species is $\text{CeO}_{1.9}$.

Total atomic oxygen present (including that in oxide and that in gas phase):

$$\left(\frac{2 \text{ moles O}_2}{\text{mole CeO}_2}\right) \left(\frac{1.14 \times 10^{-4} \text{ moles CeO}_2}{\text{min}}\right) = 2.27 \times 10^{-4} \text{ total moles O per min}$$

The amount of evolved oxygen (gas phase only):

$$\left(\frac{2.0 - 1.9 \text{ moles O (in gas)}}{2.0 \text{ moles O total}}\right) \left(\frac{2.27 \times 10^{-4} \text{ moles CeO}_2}{\text{min}}\right) = 1.14 \times 10^{-5} \text{ moles O / min in gas}$$

Total oxygen evolved in equivalent sccm pure O_2 :

$$\left(\frac{1.14 \times 10^{-5} \text{ moles O}}{\text{min}}\right) \left(\frac{1 \text{ mole O}_2}{2 \text{ moles O}}\right) \left(\frac{22.4 \text{ L O}_2}{1 \text{ mole O}_2 @ \text{STP}}\right) \left(\frac{1000 \text{ cm}^3}{\text{L}}\right) = 0.13 \text{ sccm O}_2$$

Controlled gas flows are typically 0.7 sccm Ar/5%H₂ and 0.3sccm Ar/8%O₂. Therefore, 0.13 sccm O₂ is quite significant. There's more than 5 times more oxygen evolved from the source than introduced via Ar/8%O₂ during a reactive evaporation of cerium metal.

@ 0.30 sccm Ar/8%O₂, the total O₂ flow is

$$0.30 \text{ sccm} \times 0.08 = 0.024 \text{ sccm O}_2$$

$0.13 \text{ sccm} / 0.024 \text{ sccm} = 5.3$ times more O₂ from CeO₂ source evolution than introduced during a typical reactive evaporation.

APPENDIX C: NICKEL OXIDE STABILITY DURING CeO₂ DEPOSITION

The stability of nickel oxide during a CeO₂ deposition performed in 1 sccm forming gas may be estimated using the results from Appendix B.

From Appendix B, the total amount of oxygen evolved from the source (both in CeO₂ and in the gas phase) was 2.27x10⁻⁴ moles O/min at 0.91 Å/s. At 0.46 Å/s, the rate will be halved, such that the total amount of oxygen coming from the source will be 1.14x10⁻⁴ moles O/min.

For 1 sccm forming gas (Ar/5%H₂), total moles of H₂ flowing into the chamber will be:

$$\left(\frac{1 \text{ cm}^3 \text{ Ar} / 5\% \text{ H}_2}{\text{min}}\right) \left(\frac{0.05 \text{ sccm H}_2}{1 \text{ sccm Ar} / 5\% \text{ H}_2}\right) \left(\frac{1 \text{ L}}{1000 \text{ cm}^3}\right) \left(\frac{1 \text{ mole H}_2}{22.4 \text{ L H}_2}\right) = 2.23 \times 10^{-6} \text{ moles H}_2$$

Balancing this hydrogen with the oxygen evolved from the source will allow calculation of a P_{H₂}/P_{H₂O} ratio which may be used to gauge NiO stability. Assume that ALL O₂ evolved reacts to form H₂O.

$$\frac{H_2}{H_2O} = \frac{2.23 \times 10^{-6} - X_o}{X_o} \quad X_o = \text{moles atomic oxygen from source}$$

The critical P_{H₂}/P_{H₂O} ratio for NiO stability is 10⁻².

$$1 \times 10^{-2} = \frac{2.23 \times 10^{-6} - X_o}{X_o}$$

$$1 \times 10^{-2} X_o = 2.23 \times 10^{-6} - X_o$$

$$1.01 X_o = 2.23 \times 10^{-6}$$

$$X_o = 2.21 \times 10^{-6} \text{ moles O}_2$$

If 2.21x10⁻⁶ moles O₂ (gas only, not bound in CeO_{2-x}) are introduced into the chamber per minute, NiO will form on the nickel substrate.

The stoichiometry of CeO₂ required to evolve this much O₂ may be found as follows:

$$1.14 \times 10^{-4} \text{ moles O total} - 2.21 \times 10^{-6} \text{ moles O in gas} = 1.11 \times 10^{-4} \text{ moles O for CeO}_{2-x}$$

$$\frac{1.11 \times 10^{-4} \text{ moles O}}{5.68 \times 10^{-5} \text{ moles Ce}} = 1.96$$

So if CeO_{1.96} is deposited from CeO₂ at 0.46 Å/s in 1 sccm flowing forming gas, the substrate will oxidize prior to deposition.

The calculation may also be reversed to determine the minimum flow rate of forming gas necessary to prevent oxidation of nickel during deposition. For the purpose of the calculation, a stoichiometry of CeO_{1.72}, the lowest stoichiometry for which the fluorite structure is stable, will be assumed.^{46,47} A deposition rate of 0.91 Å/s will be used. The total oxygen evolution at 0.91 Å/s was previously calculated to be 2.27x10⁻⁴ moles O/min (see appendix B).

$$\left(\frac{2.27 \times 10^{-4} \text{ moles O}}{\text{min}} \right) \left(\frac{2 - 1.72 \text{ moles O in gas}}{2 \text{ moles O total}} \right) = 3.18 \times 10^{-5} \text{ mole O / min}$$

The stability for NiO formation is $P_{H_2}/P_{H_2O} = 10^{-2}$, therefore

$$\frac{H_2}{H_2O} = 10^{-2} = \frac{X_{H_2} - 3.18 \times 10^{-5}}{X_{H_2}}$$

$$1 \times 10^{-2} X_{H_2} = X_{H_2} - 3.18 \times 10^{-5}$$

$$1.01 X_{H_2} = 3.18 \times 10^{-5}$$

$$X_{H_2} = 3.15 \times 10^{-5} \text{ mole } H_2 / \text{min}$$

$$\left(\frac{3.15 \times 10^{-5} \text{ mole } H_2}{\text{min}} \right) \left(\frac{22.4 \text{ L}}{1 \text{ mole}} \right) \left(\frac{1000 \text{ cm}^3}{1 \text{ L}} \right) \left(\frac{1 \text{ sccm Ar} / 5\% H_2}{0.05 \text{ sccm } H_2} \right) = 14.1 \text{ sccm Ar} / 5\% H_2$$

This is a far higher flow of forming gas than used during any typical deposition.

APPENDIX D: OXYGEN FLOW NECESSARY TO OXIDIZE CERIUM DURING METALLIC DEPOSITION

The flow of oxygen necessary to oxidize all the cerium metal evaporated from the source during metallic deposition may be calculated.

The deposition rate of Ce from the source must be estimated. Optical thickness measurements are not possible on films deposited from cerium metal since they are highly reduced and strongly absorbing.

Assume that when the monitor reads 0.5 Å/s, the true deposition rate is only 0.1 Å/s maximum ($R_o = 0.1 \text{ Å/s}$)

From Appendix B, the volume of material deposited per unit time is $\pi R_o r^2$.

$$R_o = \left(\frac{0.1 \text{ Å}}{\text{sec}} \right) \left(\frac{1 \text{ cm}}{1 \times 10^{-8} \text{ Å}} \right) \left(\frac{60 \text{ sec}}{\text{min}} \right) = 6 \times 10^{-8} \text{ cm/min}$$

$$\frac{\text{vol CeO}_2}{\text{min}} = \pi (6 \times 10^{-8} \text{ cm/min}) (39 \text{ cm})^2 = 2.87 \times 10^{-4} \text{ cm}^3 / \text{min}$$

Total moles Ce deposited per minute:

$$\left(\frac{2.87 \times 10^{-4} \text{ cm}^3}{\text{min}} \right) \left(\frac{6.67 \text{ g Ce}}{1 \text{ cm}^3 \text{ Ce}} \right) \left(\frac{1 \text{ mole Ce}}{140.11 \text{ g Ce}} \right) = 1.36 \times 10^{-5} \text{ moles Ce/min}$$

To form stable fluorite phase material, the stoichiometry of the CeO_{2-x} must be at least $\text{CeO}_{1.72}$.^{46,47} The amount of oxygen required to form material of this stoichiometry is:

$$\left(\frac{1.36 \times 10^{-5} \text{ mole Ce}}{\text{min}} \right) \left(\frac{1.72 \text{ mole O}}{\text{mole CeO}_{1.72}} \right) = 2.35 \times 10^{-5} \text{ mole O/min} = 1.17 \text{ mole O}_2 / \text{min}$$

$$\left(\frac{1.17 \text{ mole O}_2}{\text{min}} \right) \left(\frac{22.4 \text{ L}}{\text{mole}} \right) \left(\frac{1000 \text{ cm}^3}{1 \text{ L}} \right) = 0.26 \text{ sccm O}_2$$

The amount of oxygen flow needed to compensate the cerium metal during a metallic deposition is considerable greater than the amount of oxygen typically introduced into the chamber during a typical run (0.3 sccm Ar/8%O₂)

Ar/8%O₂:

$$\frac{0.26}{0.08} = 3.3 \text{ sccm Ar / 8\%O}_2 \text{ required}$$

Ar/40%O₂:

$$\frac{0.26}{0.40} = 0.66 \text{ sccm Ar / 40\%O}_2 \text{ required}$$

Note that while 0.26 sccm of oxygen must be introduced to oxidize the cerium metal, sufficient H₂ must also be introduced to ensure that the P_{H₂}/P_{H₂O} ratio is sufficiently high to prevent nickel oxide formation. The P_{H₂}/P_{H₂O} ratio must be higher than 10⁻², so the amount of forming gas required to prevent NiO formation is:

$$\frac{X \text{ sccm H}_2 - 2(0.26 \text{ sccm O}_2)}{2(0.26 \text{ sccm O}_2)} = \frac{P_{H_2}}{P_{H_2O}} = 10^{-2}$$

$$X \text{ sccm H}_2 - 0.52 = 5.2 \times 10^{-3}$$

$$X \text{ sccm H}_2 \approx 0.53 \text{ sccm}$$

$$\frac{0.53 \text{ sccm H}_2}{0.05} = 10.5 \text{ sccm Ar / 5\%H}_2$$

10.5 sccm Ar/5%H₂ must be mixed with this flow of oxygen to prevent Ni oxidation prior to deposition.

The calculation assumes that no substantial equilibrium exists between CeO₂ vs. H₂O formation...all oxygen reacts with cerium metal before any reacts with H₂.

BIBLIOGRAPHY

1. N.M. Alford, *Chem. Ind.* **21**, 809 (1992).
2. J.G. Bednorz, K.A. Muller, *Z. Phys. B Cond. Matter* **64**, 189 (1986).
3. M.K. Wu, J.R. Ashburn, C.J. Torng, P.H. Hor, R.L. Meng, L. Gao, Z.J. Huang, Y.Q. Wang, C.W. Chu, *Phys. Rev. Lett.* **58**[9], 908 (1987).
4. A. Goyal, D.P. Norton, D.M. Kroeger, D.K. Christen, M. Paranthaman, E.D. Specht, J.D. Budai, Q. He, B. Saffian, F.A. List, D.F. Lee, E. Hartfield, P.M. Martin, C.E. Klaubunde, J. Mathis, C. Park, *J. Mater. Res.* **12**[11], 2924 (1997).
5. O.G. Vendik, S.G. Kolesov, *J.Phys. III* **8**, 1659 (1993).
6. D. Dimos, P. Chaudhari, J. Mannhart, F.K. LeGoues, *Phys. Rev. Lett.* **61**, 219 (1988).
7. P.C. McIntyre, M.J. Cima, J.A. Smith, Jr., M.P. Siegal, J.M. Phillips, R.B. Hallock, *J. App. Phys.* **71**[4], 1868 (1992).
8. A. Goyal, D.P. Norton, M. Paranthaman, J.D. Budai, E.D. Specht, D.K. Christen, D.M. Kroeger, Q. He, B. Saffian, F.A. List, D.F. Lee, C.E. Klabunde, P.M. Martin, *Advances in Superconductivity IX: Proceedings on the 9th International Symposium on Superconductivity*, vol 2., S. Nakajima and M. Murakami, eds., Springer-Verlag, Tokyo, Japan (1997) pp 685-688.
9. M. Fukutomi, S. Aoki, K. Komori, R. Chaterjee, H. Maeda, *Physica C* **219**, 333 (1994).
10. L.S. Yu, J.M.E. Harper, J.J. Cuomo, D.A. Smith, *Appl. Phys. Lett.* **47**[9], 932 (1985).
11. Y. Iijima, N. Tanabe, O. Kohno, Y. Ikeno, *Appl. Phys. Lett.* **60**, 769 (1992).
12. X.D. Wu, S.R. Foltyn, P.N. Arendt, W.R. Blumenthal, I.H. Campbell, J.D. Cotton, J.Y. Coulter, W.L. Hulst, M.P. Maley, H.F. Safar, J.L. Smith, *Appl. Phys Lett.* **67**, 2397(1995)
13. N. Sonnenberg, A.S. Longo, M.J. Cima, B.P. Chang, K.G. Ressler, P.C. McIntyre, Y.P. Liu, *J. Appl. Phys.* **74**[2], 1027 (1993).

14. K.G. Ressler, N. Sonnenberg, M.J. Cima, *J. Am. Ceram. Soc.* **80**[10], 2637 (1997).
15. J. Wiesmann, K. Heinemann, H.C. Freyhardt, *Nucl. Instrum. Meth Phys. Res. Sec. B* **120**, 290 (1996).
16. C.P. Wang, K.B. Do, M.R. Beasley, T.H. Geballe, R.H. Hammond, *Appl. Phys. Lett.* **71**[20], 2955 (1997).
17. A. Goyal, D.P. Norton, J. Budai, M. Paranthaman, E.D. Specht, D.M. Kroeger, D.K. Christen, Q. He, B. Saffian, F.A. List, D.F. Lee, P.M. Martin, C.E. Klaubunde, E. Hartfield, V.K. Sikka, *Appl. Phys. Lett.* **69**, 1795 (1996).
18. M. Paranthaman, A. Goyal, D.P. Norton, F.A. List, E.D. Specht, D.K. Christen, D.M. Kroeger, J.D. Budai, Q. He, B. Saffian, D.F. Lee, P.M. Martin, *Advances in Superconductivity IX: Proceedings on the 9th International Symposium on Superconductivity*, vol 2., S. Nakajima and M. Murakami, eds., Springer-Verlag, Tokyo, Japan (1997) pp 669-672.
19. Q. He, D.K. Chisten, J.D. Budai, E.D. Specht, D.F. Lee, A. Goyal, D.P. Norton, M. Paranthaman, F.A. List, D.M. Kroeger, *Physica C* **275**, 155 (1997).
20. American Superconductor Corporation, Westborough, MA.
21. Applied Technologies Enterprises, Irmo, SC.
22. G. Finkenbeiner Inc., Waltham, MA.
23. Aremco Products Inc., Ossining, NY.
24. Bronwill, Rochester, NY.
25. Buehler Ltd., Lake Bluff, Illinois.
26. Olympus Corporation of America, New Hyde Park, NY.
27. SPI Supplies, West Chester, PA.
28. J.M. Ney Company, Bloomfield, CT.
29. Ernest F. Fullam, Inc., Latham, NY.

30. Advanced Ceramics Corporation, Cleveland, OH.
31. Omega Engineering, Inc., Stamford, CT.
32. Varian Vacuum Products, Lexington, MA.
33. Fil-Tech, Inc., Boston, MA.
34. Edwards High Vacuum International, Wilmington, MA.
35. Airco/Temescal, Berkeley, CA.
36. Sycon Instruments, Inc., East Syracuse, NY.
37. Alfa-Aesar, A Johnson Matthey Company, Ward Hill, MA.
38. Aldrich Chemical Company Inc., Milwaukee, WI.
39. Beckman Instruments Inc., Fullerton, CA.
40. R. Swanepoel, *J. Phys. E: Sci. Instrum.* **16**, 1214 (1983).
41. Microsoft Corporation.
42. Daniel Hyams, Starkville, MS.
43. Rigaku/USA, Danvers, MA.
44. T.B. Reed, *Free Energy of Binary Compounds: An Atlas of Charts for High Temperature Chemical Calculations*, The Massachusetts Institute of Technology, 1971.
45. C.H.P. Lupis, *Chemical Thermodynamics of Materials*, North-Holland, NY, 1983.
46. O.T. Sorenson, *J. Solid State Chem.* **18**, 217 (1976).
47. D.J.M. Bevan, J. Kordis, *J. Inorg. Nucl. Chem.* **26**, 1509 (1964).
48. R.C. Weast, ed., *CRC Handbook of Chemistry and Physics*, CRC Press, Cleveland, OH, 1975 p. A-137.